Final version is available on: https://doi.org/10.1016/j.jobe.2021.103089

Sustainable reflective triple glazing design strategies: spectral characteristics, air-conditioning cost savings, daylight factors, and payback periods

G. Kirankumar[a], S. Saboor[b*], K.J. Kontoleon[c], Domenico Mazzeo[d], M.Venkata Ramana[b], S. Sharmas Vali[e]

[a]Department of Mechanical Engineering, Sasi Institute of Technology and Engineering, Tadepalligudem - 534101, Andhra Pradesh, India.

[b]School of Mechanical Engineering, Vellore Institute of Technology, Vellore - 632014, Tamil Nadu, India.

[c] Department of Civil Engineering, Aristotle University of Thessaloniki, University Campus - Gr 54124, Thessaloniki, Greece.

[d]Department of Mechanical, Energy and Management Engineering (DIMEG), University of Calabria, 87036 Rende, Italy

[e]Department of Mechanical Engineering, National Institute of Technology Karnataka, Surathkal - 575014, Karnataka, India.

(*Corresponding Author: e-mail: saboor.nitk@gmail.com)

Abstract:

Buildings with conventional glazing systems are responsible for excessive cooling and heating costs. Sustainable use of energy in building environments requires the use of high-performing opaque and windowed walls. Triple glazing units attenuate solar heat gain/loss compared to single- and double-glazing assemblies, thus reducing air-conditioning costs and greenhouse gas emissions. The optical, energy, economic and environmental performances of a glazing unit are strictly correlated with each other. An improvement of optical properties leads to higher glazing energy performance, cost savings, and greenhouse gas emission mitigations. This work aims to suggest and define an energy-efficient triple glazing unit for lowering cooling and heating costs in buildings while experimentally testing the spectral performance of reflective glasses and assessing heat gains/losses. In this regard, bronze, green, grey, sapphire blue, and gold reflective glasses were considered and settled in sixty different triple glazing combinations. Spectral characteristics of reflective glasses were

Final version is available on: https://doi.org/10.1016/j.jobe.2021.103089

measured experimentally using a spectrophotometer over the entire solar spectral range (300-2500 nm). For the aims of this investigation, a numerical model was developed to assess the net annual cost saving ($\$/m^2$) and the payback period of the examined glazing units for the eight cardinal directions (N, N-E, E, S-E, S, S-W, W and N-W). The results confirmed that the TWG35 window glass unit in the S-E orientation was the most energy-efficient glazing in terms of alleviating this critical challenge (air-conditioning cost-saving 16.72 $\$/m^2$ among all other studied window glass units), while a payback period of 2.2 years was revealed. On the other hand, the TWG33 window glass unit has led to the optimal-lowest payback period (2.1 years), with a net annual cost saving of 16.55 $\$/m^2$. The findings of this paper demonstrate the significance of triple-glazing design approaches from an economic and environmental point of view.

Keywords: Triple glazing units; Energy conscious buildings; Air-conditioning cost-savings; Payback period; Color rendering index and daylight factor.

1. INTRODUCTION

Energy consumption in buildings has been rising radically, showing an exponential trend due to the increased demand to improve indoor ambiances by evolving opportunities for maintaining indoor thermal comfort conditions. Furthermore, domestic electricity supply escalates due to increased household energy use, electrical appliances, and human population growth. Within this framework, more than 50% of households' utilized energy is directed towards air-conditioning applications.

As is widely known, a conspicuous reduction in energy demand for air-conditioning can be attained by adopting rational building envelope schemes while applying efficient HVAC systems. The building envelope is the physical barrier between the controlled environment and the ambient air in simple terms. It becomes apparent that building components collaborate to maintain conditioned spaces comfortable for residents by regulating the heat fluxes between the interior and the exterior environments. Recently, a broad group of researchers focused their attention on studying energy-efficient envelope solutions to reduce energy consumption, greenhouse gas emissions, and climate change mitigation [1].

The building envelope energy efficiency through the glazing is associated with proper selection of glazing system, orientation, optimal glazing area (WWR), and solar-optical properties. The glazing systems contribute significantly to provide thermal and visual comfort to inhabitants within buildings. Compared to other opaque building components, the majority

Final version is available on: https://doi.org/10.1016/j.jobe.2021.103089

of solar radiation penetrates through the glazing surfaces. The properties of single-pane clear glazing, such as the thermal transmittance and solar heat gain coefficient (SHGC), affect heat flow processes through building configurations [2]. Jorge et al. proposed a method to select window glazing based on transmittance, g-values, and visible light transmittance values to reduce the building energy consumption and CO_2 emissions with adequate daylighting [3].

Transparent and Low-E double and triple-paned glazing windows were studied to reduce cooling and heating loads in building compared to conventional glazing [4]. Double and triple glazed units interspace filled with air and inert gases were studied experimentally and numerically to evaluate their solar characteristics more accurately and model the heat transfer. [5,6]. Phase change materials (PCM) are incorporated in the interspace of multi-layer glazing to mitigate and delay the heat gain through the glazing systems [7]. PCM thickness and melting temperatures were studied for their effect on the thermal performance of multi-layer glazing [8]. Window systems substituted with effective double or triple-paned glazing systems of lower or higher heat gain coefficients had concluded significant energy savings in existing residential buildings [9]. Experimental investigation of aerogel glazing system with numerical model reported a 32% annual heat gain reduction and significantly enhanced indoor illuminance [10]. Glazing with different window-wall ratios (WWR) was studied for optimum orientation and marginal heat gains across different Indian climates [11]. In another study, school buildings with varying glazing ratios were studied for occupants' visual comfort and energy demands in Turkey [12]. In the margin of the present endeavor, a mathematical model to validate the simulation results with experimental findings of the global solar radiation on glazing surfaces was developed. The model predicts the heat transfer coefficient (U-value) and the solar heat gain constants (SHGC) [13]. In the framework of another study, various combinations of glazing properties (SHGC and visible transmittance) were analyzed for optimum energy efficiency in buildings with the Quick energy simulation tool (e-QUEST) [14]. Investigations on the thermal performance of glazing in Coimbra (Portugal) concluded that triple glazing systems expose a superior performance compared to the single- and double-glazing units [15].

Reductions in energy consumption were reported with low-ε double-glazing, thermotropic, and PV window systems compared to conventional glazing [16]. Electrically actuated smart switchable glazing such as SPD, PDLCs, and Electrochromic glazing systems were extensively studied for dynamic solar control and variable transparency [17–20]. Smart window glazing showed the reductions in energy requirements for heating and cooling needs along with visual and thermal comfort. Solar glazing factors described different window glazing configurations, glass structures, and electrochromic windows for computation and comparison of glazing for heat flows in buildings [21]. Further, the power required to switch the smart glazing between opaque and transparent states can be obtained with building-integrated PVs and SPDs optimized for power loss [22]. Smart glazing with a multi-layer coating of WO_3/Cu-TiO_2 was evaluated with building energy modeling, concluded the energy savings without affecting daylighting in building interiors [23]. The effect of atmospheric clearness and sky conditions on daylight, solar energy transmission, and the performance of smart glazing was experimentally investigated [24–26]. The experimental results of insulating glazing units with double glazed windows of inter-pane blinds were also reported to determine U-value [27]. Double-glazing units with Venetian blinds at different slant positions were studied with CFD simulations to regulate heat transfer coefficients, which was an improvement of 28% compared to the base case [28]. Experimental and simulation studies of double-glazing units with inert gases (krypton, xenon) in interspace reported a reduction in building cooling loads along with adequate daylight levels [29,30]. The effect of facade orientation, glazing proportion, aspect ratio, and glazing properties over solar heat flux was assessed for the northern Greek region [31].

Furthermore, optimum designed triple-glazed windows have reported the highest energy savings in three different European latitudes than single and double-glazed window units for summer and winter [32]. DOE-2 simulations of Low-E double and triple glazed units of a residential building in Inchon and Ulsan (South Korea) found that multi-pane glazing led to improved energy and carbon footprint performance compared to clear glass double-glazing unit [33]. Various double-glazing units were studied analytically and experimentally for solar heat gain coefficients at different WWR for three different climatic conditions in Portugal [34]. The multi-pane glazing units of different tinted and reflective glasses were studied for the minimal heat gains and net annual cost savings with the Energy Plus tool for Indian climatic conditions [35–38]. Sunlit pattern and view factor methodologies were adopted through computer simulations to maximize heat gain in buildings during the winter season for Mediterranean climatic conditions [39].

The above-discussed literature reveals no significant research work on the air-conditioning cost-saving studies of buildings using reflective triple glazed window units. This study aims to investigate and underline the optimum design of triple glazing units to lower air-conditioning costs. Thus, five reflective glasses were selected in an arrangement of 60 different triple glazing configurations, and these triple glazed window units were examined for their solar optical properties (transmittance and reflectance). Solar heat gain through the various triple-glazed units was computed on peak summer and peak winter days in the eight cardinal orientations of the multifaceted climatic zone in India. A numerical model was developed to calculate the annual air-conditioning cost savings of various combinations of triple glazing compared to clear triple glazing. These results are helpful to architects and engineers who deal with the construction of energy-conscious buildings.

2. MATERIALS AND METHODOLOGY

2.1. Analyzed types of glazing panels

Five illustrative types of reflective glasses, available in the Indian market in different colors, such as Bronze (BZRGW), Green (GRGW), Grey (GrRGW), Sapphire blue (SPBRGW), and Gold (GLDRGW), were considered for this thermal analysis. As well known, the multiple glazing configurations attenuate heat flux through it compared to the single-pane glazing. In the present study, 5 mm thick reflective glasses of 30 mm x 30 mm dimensions were used to obtain triple glazing window units (**Fig. 1**). A 10 mm gap was maintained among the triple glazing glass panes with the aid of a spacer, and the overall thickness of the glass unit was shown to be 35 mm.

INSERT FIGURE

Fig. 1. Outline of a triple glazed unit consisting of reflective glasses.

For each reflective glass exposed to the outdoor environment, 12 triple glazing configurations can be formed. Therefore, a total of sixty triple window glass units (TWG1 to TWG60) were developed through the variation of the outside, middle, and inside glass panes of the triple glazing, as shown in **Fig. 2a to 2e.** The arranged triple glazed reflective window units were studied to determine the solar optical properties and the solar heat gain coefficients (SHGCs).

INSERT FIGURE

Fig. 2. Reflective triple glazing configurations with: (a) Bronze color; (b) Green color; (c) Grey color; (d) Sapphire blue color; (e) Gold color.

2.2. Experimental assessment of solar optical properties of reflective glasses

Solar optical properties of glazing serve as a basis to calculate the transmission of solar radiation through glazing. Spectral characteristics of reflective glasses were obtained with a double beam monochromatic spectrophotometer. Deuterium and tungsten-halogen lamps were used as the light sources in UV and VIS-NIR regions, respectively. Spectral transmission of samples was detected with the Photomultiplier (R-687) and Pbs detectors. The reflection from the sample beam was collected with the help of the integrating sphere. The wavelength accuracy of the spectrophotometer is ± 0.08 nm in the Ultraviolet (UV) and Visible (VIS) region and ± 0.30 nm in the Near-Infrared (NIR) region. Spectral transmission (%T) and reflection (%R) were measured for five reflective glasses in the 300 - 2500 nm wavelength range at an interval of 2 nm at a normal angle of incidence [40].

A MATLAB code was developed for Eq. (1) to calculate solar properties from measured spectral data as per British standards [41,42] and presented in **Table 1**. Solar absorptance was calculated using the relation between the solar properties i.e., summation of properties as unity ($T_{SOLAR} + R_{SOLAR} + A_{SOLAR} = 1$).

Final version is available on: https://doi.org/10.1016/j.jobe.2021.103089

$$T_{SOLAR} = \frac{\sum_{\lambda=300}^{\lambda=2500} S_\lambda \tau(\lambda)\Delta\lambda}{\sum_{\lambda=300}^{\lambda=2500} S_\lambda \Delta\lambda}, \qquad R_{SOLAR} = \frac{\sum_{\lambda=300}^{\lambda=2500} S_\lambda \rho(\lambda)\Delta\lambda}{\sum_{\lambda=300}^{\lambda=2500} S_\lambda \Delta\lambda} \tag{1}$$

INSERT TABLE

Table 1

Solar, color rendering properties and thermal indices of reflective glasses

Figs. 3a & 3b present the spectral characteristics (%T and %R) of five reflective glasses in the wavelength range of 300-2500 nm. Gold reflective glass possesses a high spectral transmission and reflection in the entire wavelength range. The grey reflective glass showed the lowest spectral reflection in the whole wavelength range.

INSERT FIGURE

Fig. 3. Spectral characteristics of reflective glasses.

2.3 Color rendering of daylight through various reflective glasses

The general color rendering index (R_a) and correlated color temperature (CCT) of building interior daylight were evaluated to know the color quality of transmitted daylight through reflective glasses used in triple glazing units of the current study. The R_a and CCT are quantitative metrics used to justify the color rendering and quality of daylight. CIE standard illuminant D_{65} was used as reference illuminant for analysis. Color rendering properties of incoming daylight through the single-pane reflective glasses were computed following British standard [42].

Tristimulus values of transmitted light (X_t, Y_t, Z_t) through reflective glasses and reflected light by each of eight test colors ($X_{t,i}$, $Y_{t,i}$, $Z_{t,i}$) are given by Eqs. (2)-(4).

$$X_t = \sum_{\lambda=380\text{ nm}}^{\lambda=780\text{ nm}} D_{65}(\lambda)\,\tau(\lambda)\bar{x}(\lambda)\Delta\lambda, \qquad X_{t,i} = \sum_{\lambda=380\text{ nm}}^{\lambda=780\text{ nm}} D_{65}(\lambda)\,\tau(\lambda)\,\beta_i(\lambda)\,\bar{x}(\lambda)\,\Delta\lambda \tag{2}$$

$$Y_t = \sum_{\lambda=380\text{ nm}}^{\lambda=780\text{ nm}} D_{65}(\lambda)\tau(\lambda)\,\bar{y}(\lambda)\,\Delta\lambda, \qquad Y_{t,i} = \sum_{\lambda=380\text{ nm}}^{\lambda=780\text{ nm}} D_{65}(\lambda)\,\tau(\lambda)\,\beta_i(\lambda)\,\bar{y}(\lambda)\,\Delta\lambda \tag{3}$$

$$Z_t = \sum_{\lambda=380\text{ nm}}^{\lambda=780\text{ nm}} D_{65}(\lambda)\tau(\lambda)\,\bar{z}(\lambda)\,\Delta\lambda\,, \qquad Z_{t,i} = \sum_{\lambda=380\text{ nm}}^{\lambda=780\text{ nm}} D_{65}(\lambda)\,\tau(\lambda)\,\beta_i(\lambda)\,\bar{z}(\lambda)\,\Delta\lambda \tag{4}$$

Where D_{65} (λ) is the relative spectral power distribution of CIE standard illuminant D_{65}

$\tau(\lambda)$ is measured spectral transmittance of reflective glasses

$\bar{x}$ (λ), $\bar{y}$ (λ), and $\bar{z}$ (λ) are the spectral tristimulus values for CIE-1931

$\Delta\lambda$ is the wavelength interval (10 nm)

and $\beta_i(\lambda)$ is the spectral reflectance of each test color, i (i=1 to 8)

Trichromatic co-ordinates for the transmitted light (u_t, v_t) and test color reflected light ($u_{t,i}$, $v_{t,i}$) were calculated using Eqs. (5) & (6).

$$u_t = \frac{4X_t}{(X_t + 15\,Y_t + 3Z_t))}\,, \qquad v_t = \frac{6Y_t}{(X_t + 15\,Y_t + 3Z_t))} \tag{5}$$

$$u_{t,i} = \frac{4X_{t,i}}{(X_{t,i} + 15\,Y_{t,i} + 3Z_{t,i})}\,, \qquad v_{t,i} = \frac{6Y_{t,i}}{(X_{t,i} + 15\,Y_{t,i} + 3Z_{t,i})} \tag{6}$$

Corrected trichromatic co-ordinates in terms of distortion by the chromatic adaptation for eight test colors were calculated with Eqs. (7) & (8).

$$u'_{t,i} = \frac{10.872 + 0.8802\,\frac{c_{t,i}}{c_t} - 8.2544\,\frac{d_{t,i}}{d_t}}{16.518 + 3.2267\,\frac{c_{t,i}}{c_t} - 2.0636\,\frac{d_{t,i}}{d_t}} \tag{7}$$

$$v'_{t,i} = \frac{5.520}{16.518 + 3.2267\,\frac{c_{t,i}}{c_t} - 2.0636\,\frac{d_{t,i}}{d_t}} \tag{8}$$

Where c_t, d_t are for transmitted light and $c_{t,i}$, $d_{t,i}$ for each test color i, calculated using Eqs. (9) & (10) respectively.

$$c_t = \frac{4 - u_t - 10\,v_t}{v_t}\,, \qquad d_t = \frac{1.708\,v_t + 0.404 - 1.481\,u_t}{v_t} \tag{9}$$

$$c_{t,i} = \frac{4 - u_{t,i} - 10\,v_{t,i}}{v_{t,i}}\,, \qquad d_{t,i} = \frac{1.708\,v_{t,i} + 0.404 - 1.481\,u_{t,i}}{v_{t,i}} \tag{10}$$

Final version is available on: https://doi.org/10.1016/j.jobe.2021.103089

Trichromatic co-ordinates were converted into uniform color space systems ($U^*_{t,i}$, $V^*_{t,i}$, $W^*_{t,i}$); the following Eqs. (11)-(13) were used for each test color conversion.

$$W^*_{t,i} = 25\left(\frac{100\ \mathrm{Y_{t,i}}}{\mathrm{Y_t}}\right)^{1/3} - 17 \tag{11}$$

$$U^*_{t,i} = 13\ W^*_{t,i}\ (\mathrm{u'}_{\mathrm{t,i}} - 0.1978) \tag{12}$$

$$V^*_{t,i} = 13\ W^*_{t,i}\ (\mathrm{v'}_{\mathrm{t,i}} - 0.3122) \tag{13}$$

The total distortion (ΔE_i) of each test color i, was determined as follows

$$\Delta \mathrm{E_i} = \sqrt{\left(U^*_{t,i} - U^*_{r,i}\right)^2 + \left(V^*_{t,i} - V^*_{r,i}\right)^2 + \left(W^*_{t,i} - W^*_{r,i}\right)^2} \tag{14}$$

The CIE standard illuminant D_{65} values for the test colors ($U^*_{r,i}$, $V^*_{r,i}$, $W^*_{r,i}$) were calculated for daylight inflow through the opening without glazing.

The specific color rendering index (R_i) of each test color i, was determined from Eq. 15.

$$\mathrm{R_i} = 100 - 4.6\ \Delta \mathrm{E_i} \tag{15}$$

The general color rendering index (R_a) of the daylight in building interiors through the reflective glasses was calculated using Eq. (16).

$$\mathrm{R_a} = \frac{1}{8}\sum_{i=1}^{8} \mathrm{R_i} \tag{16}$$

The correlated color temperature (CCT) was calculated with the help of McCamy's cubic approximation (Eq. 17).

$$\mathrm{CCT} = -449\ \mathrm{n}^3 + 3525\ \mathrm{n}^2 - 6823.3n + 5520.33 \tag{17}$$

Where $\mathrm{n} = \frac{\mathrm{x} - 0.3320}{\mathrm{y} - 0.1858}$, in which $\mathrm{x} = \frac{\mathrm{X}_t}{\mathrm{X}_t + \mathrm{Y}_t + Z_t}$ and $\mathrm{y} = \frac{\mathrm{Y}_t}{\mathrm{X}_t + \mathrm{Y}_t + Z_t}$

The color rendering index (R_a) and correlated color temperature (CCT) of five reflective glasses were evaluated and presented in **Table 1**. For indoor illumination, rendering metric R_a > 80 and a CCT with the range of 3000-5500 K will be perceived as good rendering, and R_a > 90 will be a very good rendering [43,44]. The R_a metric of all glass samples was well above the minimum recommended level as per the CIE standards for good color rendering. It is observed that Grey reflective glass had reported the highest R_a of 93.42 and bronze reflective glass a lowest R_a of 80.18. The CCT of all reflective glasses was in the range of 5100-5375 K, representing strong cool daylight. The high R_a metric and CCT of studied reflective glasses assures the vibrant and natural daylight inflow through triple glazing units in building interiors and avoid the need for artificial daylighting. Spectral transmittance of the glass samples significantly affects the color rendering properties of the daylight. A constant transmittance in the visible region was required for good rendering properties of daylight.

The Five reflective glasses were arranged in 60 possible triple glazing combinations and the solar optical properties of triple glazing units were obtained as per the methodology presented in CIBSE Guide [45]. Solar heat gain coefficients (SHGC) serve as a basis for solar heat gain/loss calculations through glazing. SHGC of the triple glazing ($SHGC_{TWG}$) can be computed with the following correlation in Eq. (18) and tabulated in **Table 2**.

$$\mathbf{SHGC_{TWG}} = \left(\mathbf{T_{SOL,TWG}} + \mathbf{U_3} \left(\frac{\mathbf{A_o^1 + A_c^1 + A_i^1}}{\mathbf{h_o + h_i}} + \left(\mathbf{A_o^1 \cdot 2C_{ag}} \right) \right) \right) \tag{18}$$

Where;

$\mathbf{T_{SOL,TWG}}$ is the solar transmittance of the triple glazing unit, and it can be computed using Eq. (20).

A_o^1, A_c^1, and A_i^1 solar absorptance of outside, center, and inside glass panes and obtained from Eqs. (21) to (23).

In addition, C_{ag} is the thermal resistance of the air gap in the interspace of multiple glazing, as presented in Eq. (19):

$U_3$is unsteady-state thermal transmittance of triple glazing unit:

$$C_{ag} = 1 \Bigg/ \left(1.25 + \left(2.32 \cdot \left(\sqrt{\left(1 + \left(\frac{{t_{ag}}^2}{{w_{ag}}^2} \right) \right)} - \frac{t_{ag}}{w_{ag}} \right) \right) \right) \tag{19}$$

$$T_{SOL,TWG} = \frac{(T_e \times T_m \times T_i)}{\left(\left(1 - (R_e \times R_m) \right) \times \left(1 - (R_m \times R_i) \right) - (T_m^2 \times R_e \times R_i) \right)} \tag{20}$$

Final version is available on: https://doi.org/10.1016/j.jobe.2021.103089

$$A_o^1 = A_e + \left[(T_e \times A_e \times R_m)/\left(1 - (R_e \times R_m)\right)\right] + (T_e {T_m}^2 A_e R_i/\left(\left(1 - (R_e \times R_m)\right) \times \left(1 - (R_m \times R_i)\right) - (T_m^2 \times R_e \times R_i)\right)) \tag{21}$$

$$A_c^1 = [(T_e \times A_m)(1 - (R_e R_i) + T_m \times R_i] + ((T_e {T_m}^2 A_e R_i)/\left(\left(1 - (R_e \times R_m)\right) \times \left(1 - (R_m \times R_i)\right) - (T_m^2 \times R_e \times R_i)\right)) \tag{22}$$

$$A_i^1 = [(T_e \times T_m \times A_i] + ((T_e {T_m}^2 A_e R_i)/\left(\left(1 - (R_e \times R_m)\right) \times \left(1 - (R_m \times R_i)\right) - (T_m^2 \times R_e \times R_i)\right)) \tag{23}$$

$\mathbf{U_3}$ in Eq. (18) is the unsteady thermal transmittance *(U-value)* of the triple glazing unit, evaluated by solving 1-D heat diffusion equation with the help of transmission matrix of multiple glazing layers and air-gaps as shown in Eq. (24)

$$\begin{bmatrix} M_1 & M_2 \\ M_3 & M_4 \end{bmatrix} = \begin{bmatrix} 1 & -{h_i}^{-1} \\ 0 & 1 \end{bmatrix} \begin{bmatrix} m_1 & m_2 \\ m_3 & m_1 \end{bmatrix} \begin{bmatrix} 1 & -C_{ag} \\ 0 & 1 \end{bmatrix} \begin{bmatrix} n_1 & n_2 \\ n_3 & n_1 \end{bmatrix} \begin{bmatrix} 1 & -C_{ag} \\ 0 & 1 \end{bmatrix} \begin{bmatrix} o_1 & o_2 \\ o_3 & o_1 \end{bmatrix} \begin{bmatrix} 1 & -{h_e}^{-1} \\ 0 & 1 \end{bmatrix} \tag{24}$$

The external (h_e) and internal (h_i) heat transfer coefficients were taken as 25.00 W/m^2 K and 7.70 W/m^2 K, respectively, as per the standards [45].

Here, the element of each glass layer can be computed using Eq. (25).

$$\begin{bmatrix} \cosh(c + ic) & (\sinh(c + ic))/a \\ a \cdot \sinh(c + ic) & \cosh(c + ic) \end{bmatrix} \tag{25}$$

In Eq. (25), i is the imaginary number (i^2= -1). c is the cyclic thickness of glazing, and a is the characteristic admittance of the glazing, defined in Eq. (26).

$$c = (\sqrt{\pi \rho C_p/(k.P)}\ .\ t), \qquad a = \sqrt{2\pi k \rho c_p/P} \tag{26}$$

Where t is the glazing thickness

Eq. (26) incorporates all thermo-physical properties of glazing. ρ, C_p, and k are density (kg/m^3), heat capacity (J/kg·K), and thermal conductivity (W/m·K) of glazing. P is the period of cyclic energy transfer. Unsteady transmittance (U_3) of the triple glazing unit can be calculated using Eq. (27).

$$U_3 = \left|\frac{1}{M_2}\right| \tag{27}$$

Solar reflectance of triple glazed unit ($R_{SOL,TWG}$) can be evaluated using the following Eq. (28).

$$R_{SOL,TWG} = 1 - T_{SOL,TWG} - A_e^1 - A_m^1 - A_i^1 \tag{28}$$

INSERT TABLE

Table 2

Solar heat gain coefficients (SHGCs) of all reflective triple glazed units (TWG1 to TWG60)

3. Mathematical Model

An Indian composite climatic zone (Nagpur, 21.15^0N 79.09^0E) was considered and analyzed for heating, cooling, and net annual cost savings of buildings in the current work. A hypothetical building was modeled with a 16 m^2 floor area (4 m x 4 m), 3.5 m height, and 40 % WWR. As per 40% WWR [46], the window was modeled with 2.8 x 2 m dimensions. The analysis was carried out in day time between 6: 00 am-6: 00 pm (LAT) during summer and from 7: 00 am-5:00 pm (LAT) during the winter season [47-49].

3.1. Solar energy calculations

The total radiation falling on the surface of a building is the sum of direct, diffuse, and ground-reflected radiation. Heat gain in the buildings depends on several solar geometric angles such as Earth-Sun angles (Latitude, declination, and hour angle) and Sun-Surface angles (Incidence angle and surface azimuth). The following procedure is adopted to define the total heat gain and the net annual cost savings in buildings through triple-glazed window systems [50,51]. The anisotropic clear-sky model was considered at atmospheric conditions. The fundamental and derived solar angles can be calculated from the following equations.

The declination angle (d_{ia}) is given by the following Eq. (29).

Final version is available on: https://doi.org/10.1016/j.jobe.2021.103089

$$\mathbf{d_{ia} = 23.45 sin \frac{360(284 + n_d)}{365}} \tag{29}$$

Solar altitude angle (β) can be obtained from Eq. (30).

$$\mathbf{sin\beta = cosl \cdot cosd_{ia} \cdot cosh + sinl \cdot sind_{ia}} \tag{30}$$

To compute the solar azimuth angle (ϕ) and surface azimuth angle, the below Eq. (31) is used, while surface azimuths for various glass orientations are presented in **Table 3**.

$$\cos\phi = \frac{\sin\beta \cdot \sin l - \sin d_{ia}}{\cos\beta \cdot \cos l}, \qquad \gamma = \Phi - \Psi \tag{31}$$

INSERT TABLE

Table 3

Surface azimuths (0^{o} to ± 180^{0}) for different orientations taken from the south [52].

The below Eq. (32) gives the incidence angle (θ):

$$\mathbf{cos\theta = cos\beta \cdot cos\gamma \cdot cosk - sin\beta \cdot sink} \tag{32}$$

Solar irradiance (I_{DN}) on the earth surface for a clear day and direct sun's energy (I_{DSR}) incident on the glazing surface can be obtained with Eq. (33).

$$I_{DN} = \frac{A_1}{\exp(B_1/\sin\beta)} \qquad I_{DSR} = I_{DN} \cdot \cos\theta \tag{33}$$

The diffused energy (I_{dSR}) incident on the glazing and solar heat reflected onto the glazing from the ground (I_{GRD}) can be computed by Eq. (34).

$$I_{dSR} = C_1 \cdot I_{DN} \cdot \frac{1 - \sin k}{2} \qquad I_{GRD} = (C_1 + \sin\beta) \cdot I_{DN} \cdot \rho_g \cdot \left(\frac{1 - \sin k}{2}\right) \tag{34}$$

Thus, the total solar energy (I_T) incident on a window glazing is the sum of all three components of solar radiation (Direct + diffuse + ground reflected), as given in Eq. (35):

$$I_T = (I_{DSR} + I_{dSR} + I_{GRD}) \tag{35}$$

Final version is available on: https://doi.org/10.1016/j.jobe.2021.103089

The total solar energy passing through triple glazed window units can be calculated using Eq. (36).

$$I_{TRTWG} = I_T \text{ x } SHGC_{TWG} \text{ x } A_G \tag{36}$$

3.2. Cost analysis procedure

Annual cost savings is a useful parameter to justify the energy-saving potential of the glazing. Glazing that reduces heat gain in the summer is also responsible for lower heat gain in winter, which is an undesirable phenomenon. Annual cost savings reveal the net cost savings of triple glazing per year, including reducing the cooling costs in summer and increasing the heating costs in winter. Cost analysis was carried out for all the triple reflective window glass units (TWG1 to TWG60) for an Indian composite climatic zone (Nagpur) in eight orientations. Summer conditions prevail from April to August, whereas winter from September to March. The following procedure is followed to compute the net annual cost savings [53]. Solar radiation incident on glazing during the summer period ($Q_{sol,\ sum}$) can be calculated using Eq. (37), while for the winter period Eq. (38) is applied:

$$Q_{sol,sum} = (q_{ds} \cdot 30)_{Apr} + (q_{ds} \cdot 31)_{May} + (q_{ds} \cdot 30)_{Jun} + (q_{ds} \cdot 31)_{Jul} + (q_{ds} \cdot 31)_{Aug} \tag{37}$$

$$\mathbf{Q_{sol,win}} = (\mathbf{q_{dw}} \cdot \mathbf{30})_{\mathbf{Sep}} + (\mathbf{q_{dw}} \cdot \mathbf{31})_{\mathbf{Oct}} + (\mathbf{q_{dw}} \cdot \mathbf{30})_{\mathbf{Nov}} + (\mathbf{q_{dw}} \cdot \mathbf{31})_{\mathbf{Dec}} + (\mathbf{q_{dw}} \cdot \mathbf{31})_{\mathbf{Jan}} + (\mathbf{q_{dw}} \cdot \mathbf{29})_{\mathbf{Feb}} + (\mathbf{q_{dw}} \cdot \mathbf{31})_{\mathbf{Mar}} \tag{38}$$

Where q_{ds} (kW) is the average daily solar energy incident on the glazing during the summer months and q_{dw} (kW) is the average daily solar energy incident on the glass in the winter months.

To assess the decreased heat gain through triple glazing that contributes to reducing the cooling load in the summer period and the rise in heating load during the winter period, Eqs. (39) and (40) are adopted:

$$\text{Reduction in cooling load } (Q_{Red}) = Q_{sol,sum} \cdot A_G \cdot (SHGC_{TCGW} - SHGC_{TWG}) \tag{39}$$

$$\text{Increase in heating load } (Q_{Inc}) = Q_{sol,win} \cdot A_G \cdot (SHGC_{TCGW} - SHGC_{TWG}) \tag{40}$$

Where, $SHGC_{TCGW}$ and $SHGC_{TWG}$ are SHGCs of clear glass triple glazing and the reflective glass triple glazed units.

The solar transmittance, reflectance, and absorbance of clear glass triple-glazed systems were calculated as 56 %, 17 %, and 17 %, respectively, while SHGC of the triple clear glass window unit was calculated as 0.672. Unit electricity and natural gas cost costs were respectively considered $ 0.07 and $ 0.015 per kWh, as per the Indian scenario, and converted to US Dollars ($) at the current market exchange rate [54]. The CoP of the air-conditioning system and efficiency of the heating system (furnace) were taken as 2.5 and 80%, respectively. Cooling cost savings and the rise in heating costs are given in Eqns. (41) & (42) respectively, while net annual cost savings are calculated from Eq. (43):

$$\text{Cooling costs savings (\$)} = \frac{(\,Q_{Red} \cdot \text{Electricity price})}{\text{CoP of cooling system}} \tag{41}$$

$$\text{Rise in heating costs (\$)} = \frac{(Q_{Inc} \cdot \text{Fuel price})}{\text{Heating system efficiency}} \tag{42}$$

$$\text{Net annual cost savings (\$)} = \text{Cooling costs savings} - \text{Rise in heating costs} \tag{43}$$

The cost payback period is the time required to acquire the glazing implementation cost, which is derived from Eq. (44).

$$\text{Cost payback period (years)} = \frac{\text{Cost of implementation (\$)}}{\text{Net annual cost savings (\$/year)}} \tag{44}$$

At last, Eq. (45) refers to the glazing implementation cost of this suggested procedure:

$$\text{Implementation cost (\$)} = \left(\text{Triple glaz. price}\left(\frac{\$}{m^2}\right) \text{x Glaz. area } (A_G, m^2)\right) \tag{45}$$

4. RESULTS AND DISCUSSIONS

4.1. Total heat gain through triple bronze reflective glass window units of buildings during peak summer and winter days

The total heat gain through bronze reflective triple glazed units was computed for peak summer and peak winter days for the Indian composite climatic zone (Nagpur) in all orientations, and the results are shown in **Fig. 4**. In bronze reflective window glass units (TWG1 to TWG12), the bronze reflective glass pane was exposed to the outside environment, while middle and inside glass panes were varied with other reflective glasses to get the various configurations of the triple glazing (**Fig. 2a**). Heat gain through all triple bronze reflective glass window combinations is minimum in the south direction during peak summer (**Fig. 4a**) due to the sun movement from North-East to North-West direction. On the other hand, solar heat gain is maximum in the southern direction during peak winter (**Fig. 4b**) due to the sun path from South-East to South-West. The TWG3 combination in the south orientation is responsible for the lowest heat gain of 1.97 kW during summer. Among all other studied bronze reflective glass combinations, the TWG9 one is responsible for the highest heat gain of 7.23 kW in the south orientation during winter.

INSERT FIGURE

Fig. 4. Solar heat gain through triple bronze reflective glass window units.

4.2. Annual cost savings of triple bronze reflective glass window units

Cost analysis was carried out for various triple bronze reflective window glass units (TWG1 to TWG12) to compute annual cost savings ($/m^2) in comparison with the triple clear glass window unit (TCGW) for the Indian composite climatic zone in all eight orientations (**Fig. 5**). The net annual cost saving (Cooling cost + Heating cost) is the measure of the energy efficiency of the glazing. All bronze reflective glass window units have shown the highest annual cost savings in the South-East (SE) direction and the lowest in the West direction. When glazing was placed in the SE, S, and SW directions, better annual cost savings were obtained. Among all other studied triple glass units (TWG1 to TWG12) compared to the clear triple glazing, the TWG3 window glass unit, in the South-East direction, is the most energy-efficient glazing configuration that leads to the highest annual cost savings (14.88 $/m^2).

INSERT FIGURE

Fig. 5. Annual air-conditioning cost savings of triple bronze reflective glass window units in all orientations.

4.3. Total heat gain through triple green reflective window glass units of buildings during peak summer and winter days

The total heat gain (kW) through triple green reflective glass window units (TWG13 to TWG24) of buildings in eight directions during peak summer and winter days was calculated for Nagpur city and presented (**Fig. 6**). Green reflective triple glazed window units (**Fig. 2b**) are formed such that the green reflective glass pane is exposed to the outside environment, while middle and inside glass panes varied with other reflective glasses. This graph also shows that all the green reflective triple glazed window units appear to have the lowest heat gain during summer and the highest heat gain in winter in the south direction. The TWG14 window glass unit is responsible for the lowest heat gain of 1.61 kW during summer when placed in the south orientation. In winter, glazing should allow more radiation through the glazing to reduce the heating load. Thus, the TWG18 window glass unit seems to be the best, with the highest heat gain of 5.70 kW during this season.

INSERT FIGURE

Fig. 6. Total heat gain (kW) through triple green reflective glass window units in buildings in all orientations during (a) Peak summer (b) Peak winter.

4.4. Annual cost savings of triple green reflective glass window units

Fig. 7 presents the graph of the annual cost savings (\$/ m^2), in all eight orientations, for the studied combinations of triple green reflective glass window units (TWG13 to TWG24). It is concluded that all green reflective window glass units have shown the highest cost savings (\$/m^2) in the South-East direction. Compared to other studied orientations, the west-oriented window unit has shown the lowest annual cost savings (\$/m^2). The TWG14 window glass unit seems to be the most energy-efficient configuration in the South-East direction, with the highest annual cost saving (16.05 \$/m^2). Also, this configuration, in comparison to the other triple-glazed ones, has shown the highest yearly cost savings in all the studied orientations. All the green reflective triple glazed units have shown higher annual cost savings in SE, S, SW orientations than other orientations, and the difference in annual cost savings in these directions was negligible. There are no significant yearly cost savings (\$/m^2) for glazing placed in the East and West directions for all triple glazed units.

Final version is available on: https://doi.org/10.1016/j.jobe.2021.103089

INSERT FIGURE

Fig. 7. Annual air-conditioning cost savings of triple green-reflective glass window units in all orientations.

4.5. Total heat gain through triple grey reflective glass window units of buildings during peak summer and winter days

The total heat gain through grey triple reflective glass window units of buildings in eight orientations for an Indian composite climatic zone (Nagpur) during peak summer and winter days is depicted in **Fig. 8**. Grey reflective window glass units were formed such that the grey reflective glass pane was exposed to the outside environment, while middle and inside glass panes varied with other reflective glasses. All south-oriented grey triple reflective glass window units have shown the lowest heat gain in summer; the TWG35 window unit was responsible for the lowest heat gain of 1.40 kW (**Fig. 8a**). The reduced heat gain through these glazing units contributes to a decrease in cooling load in summer. In winter (**Fig. 8b**), all south-oriented window glass units have exhibited a high heat gain due to the sun path from South-East to South-West in winter. It was found that the TWG26 and TWG27 window configurations have the highest heat gain of 4.97 kW, compared to all the other studied ones.

INSERT FIGURE

Fig. 8. Total heat gains through triple grey reflective window glass units in buildings in all orientations during (a) Peak summer (b) Peak winter.

4.6. Annual cost savings of triple grey reflective glass window units

In **Fig. 9,** the net cost savings ($\$/m^2$) of triple grey reflective glass window units (TWG25 to TWG36) in all orientations compared to the clear glass triple glazing are presented. It was observed that among other reflective glass combinations, all the grey reflective window units had shown the highest annual cost savings, with the one in the South-East orientation having the highest annual cost savings ($\$/m^2$). However, the TWG35 window unit in this orientation seemed to be the most energy-efficient, with the highest annual cost savings (16.72 $\$/m^2$). There are no appreciable annual cost savings for all glazing placed in East and West directions. It can be noticed that all the grey reflective triple glazed window units have high annual cost savings in the SE, S, and SW directions, though the difference in the cost savings in these directions is negligible. The preference order of the orientation to place the glazing from the most energy-efficient to the least is SE < SW < S < N < NE = NW < E < W.

INSERT FIGURE

Fig. 9. Annual air-conditioning cost savings ($/m^2) of triple grey reflective glass window units in all orientations.

4.7. Total heat gain through triple sapphire blue reflective glass window units of buildings during peak summer and winter days

Fig. 10 shows the total heat gain (kW) through sapphire-blue triple reflective glass window units (TWG37 to TWG48) of buildings in eight orientations at peak summer and winter days for an Indian composite climatic zone. Sapphire blue reflective glass window units were designed to expose the sapphire blue reflective glass pane to external surroundings. As for the middle and internal glass panes, they were varied with other reflective glasses. All triple sapphire blue reflective glass window units in the south have exposed marginal heat gains in summer (**Fig. 10a**), while the TWG44 window glass unit has the lowest heat gain of 2.23 kW. In winter, all the south-oriented triple sapphire blue reflective window glass units result in higher heat gains than other orientations (**Fig. 10b**). Among the other studied glazing units, the TWG39 one has shown the highest heat gain of 7.77 kW in the south during the winter.

INSERT FIGURE

Fig. 10. Total heat gain through triple sapphire blue reflective window glass units in buildings.

4.8. Annual cost savings of triple sapphire blue reflective window glass units

In Fig. 11, the graphs for the annual cost savings ($/m^2), in eight cardinal directions, are given for the triple sapphire-blue reflective glass window units (TWG37 to TWG48), as compared to the triple clear ones. All sapphire-blue reflective glass window units highlight the highest annual cost savings in the South-East orientation. The South-East oriented TWG44 window unit was the most energy-efficient glazing having the highest annual cost savings (14.10 $/m^2) in all orientations. Glazing placed in the SE, S, and SW orientations leads to higher annual cost savings ($/m^2) than other orientations. The difference in the cost savings in these orientations was negligible. There are no considerable annual cost savings for all the sapphire blue reflective glazed units in the East and West directions. The preference order of orientation to place the glazing from the highest annual cost savings to the lowest is SE < SW < S < N < NE = NW < E < W.

INSERT FIGURE

Fig. 11. Annual air-conditioning cost savings of triple sapphire blue-reflective window units in all orientations.

4.9. Total heat gain through triple gold reflective glass window units during peak summer and winter days

Fig. 12 presents the total heat gain in buildings through triple gold reflective glass window units (TWG49 to TWG60), in eight orientations, for peak summer and winter days in an Indian composite climatic zone (Nagpur). In gold reflective glass window units (**Fig. 2e**), the gold reflective glass pane was exposed to the outside environment, while the middle and inside glass panes varied with other reflective glasses. As shown in **Fig. 12a** and **12b**, all triple gold reflective glass window units have marginal heat gains in summer and higher heat gains in winter in the south orientation compared to the other directions. TWG54 and TWG60 window glass units were responsible for the lowest (3.16 kW) and highest heat gains (10.89 KW), respectively, during summer and winter in this orientation. As expected, the reduced heat gain through the glazing in the summer days leads to a lower cooling load.

INSERT FIGURE

Fig. 12. Solar heat gain through the triple gold reflective glass window in buildings.

4.10. Annual cost savings of triple gold reflective glass window units

Fig. 13 depicts the graph of the annual cost savings ($\$/m^2$), in all orientations, for the triple gold reflective window glass units (TWG49 to TWG60) as compared to the triple clear glass window unit. It is observed that all South-East oriented triple gold reflective window glass units have shown the highest annual cost savings ($\$/m^2$). South-East oriented TWG54 window glass unit seemed to be the most energy-efficient underlining the highest annual cost savings (11.18 $/m^2), compared to all the other studied glazing has shown the highest yearly cost savings in all orientations. All gold reflective glass window units have shown higher annual cost savings in SE, S, and, SW directions and the difference in the cost savings in these directions is negligible.

INSERT FIGURE

Fig. 13. Annual air-conditioning cost savings of triple gold reflective glass window units in all orientations.

4.11. Operational energy, net annual cost savings, and operational energy to initial cost ratio

The operational energy (kWh) of air-conditioning system for the entire year and net annual cost savings ($) of triple glazing units in S-E orientation were calculated and presented in **Fig. 14.** The glazing with low operational energy will eventually project high net annual cost savings. It is observed that TWG 35 glazing unit had reported the lowest operational energy and the highest net annual cost savings. The highest reduced solar heat gains/loss through the TWG 35 triple glazing unit were attributed to the low operational energy of the corresponding glazing.

Fig. 14. Operational energy and Net annual cost savings of triple glazing units in S-E orientation

The ratios of operational energy (kWh) to initial cost (C_{in}) were presented in **Fig. 15,** with various triple glazing units in S-E orientation. The initial cost of the glazing will vary in the context of the location and supply, so the ratios are presented for various initial costs. The glazing cost was considered in the range of 0.8 to 1.4 times of initial cost (C_{in}) of glazing to represent ratios. It is seen that a decrease in ratio with an increase in the initial cost of gazing. The TWG 34 glazing unit reported the lowest operational energy to initial cost ratio due to a high initial cost and low operational energy.

Fig. 15. Operational energy and initial cost ratios of triple glazing units in S-E orientation

Final version is available on: https://doi.org/10.1016/j.jobe.2021.103089

4.12. Cost Payback Period of various reflective triple glazed window units

The cost payback period is calculated to know the length of time required to recover the implementation cost of triple reflective window glass units in the place of conventional glazing units. All the reflective triple glazed window units had shown the highest annual cost savings when the glazing was placed in the South-East (SE) orientation. The cost payback period was calculated for all the triple glazed window units (TWG1 to TWG60) in the South-East orientation and presented in **Fig. 16**. The implementation and saving costs have been presented in Table 4. TWG24, TWG28, and TWG33 window glass units were responsible for the lowest payback period of 2.1 years, while the TWG60 unit was found to have the highest payback period of 4.5 years with the lowest annual cost savings (9.83 \$/m^2). The Payback period was directly proportional to the annual cost savings of the respective glazing. The TWG35 window glass unit shows the highest annual cost savings (16.71 \$/m^2) among all other studied glazings with a payback period of 2.2 years. However, it must be considered that despite its highest annual cost savings, the payback period is slightly higher because of its high initial implementation cost as compared to TWG24, TWG28, and TWG33 window glass units. The implementation cost is the lowest (34 \$/m^2) for a TWG3 window glass unit with annual cost savings and a payback period of 14.90 (\$/m^2) and 2.3 years, respectively. The preferred orientation of triple glazing from highest annual cost savings to the lowest is SE < SW < S < N < NE = NW < E < W.

INSERT TABLE

Table 4
Implementation and cost savings of various triple-glazed reflective glass window units in the SE orientation

INSERT FIGURE

Fig. 16. The payback period for triple glazed reflective window units (TWG1 to TWG60) in the S-E orientation.

4.13. Average Daylight factor of Triple glazing window units in Southeast orientation of Composite Climatic Zone

The daylight factor for all triple glazing windows for the best air-conditioning cost-saving orientation is shown in **Fig. 17.** Daylighting is a natural source of light, and it is required in sufficient quantity to provide healthy day internal illuminance for the occupants. Natural daylight is essential for buildings to have visual comfort and reduce artificial daylighting power consumption. Glazing allows daylight from outside to inside, but it also allows heat to enter the buildings. Therefore, a suitable glass window must be selected to reduce heat gain by providing adequate illuminance levels inside the buildings recommended by CIE standards. Design-Builder with Energy Plus 8.9 version simulation tool was used to compute the building's average daylight factor. Average daylight factor simulation was carried out for the building of the composite climatic zone (Nagpur city). For the simulation of the average daylight factor on peak summer and winter days, the diurnal hours from 8 AM to 5 PM were considered. The average daylight factor values were recorded inside the building at the height of 0.75 m from the floor from southeast-oriented window glass. The recommended average daylighting factor for living rooms, bedrooms, office inquiry rooms, library stack rooms, and for most of the rooms is more than 0.625 as per the Indian standards. From the results, it is clear that the average daylight factor of all sixty triple glazing windows in the south-east orientation is higher than the recommended average daylight factor of 0.625 in both summer and winter seasons. The triple-glazed window units with high daylighting are recommended for reading rooms, hospitals, and pathological laboratory buildings. In contrast, low daylight triple glazed units are recommended for living rooms, stack rooms, and general office buildings.

INSERT FIGURE

Fig. 17. Average daylight factor of triple window glazing units in the south-east orientation.

5. CONCLUSIONS

The simple triple glazing design strategies result in significant air-conditioning cost savings in energy-conscious buildings. In this paper, thermal analysis of air-filled reflective triple glazed window systems (TWG1 to TWG60) was carried out for an Indian composite climatic zone in the eight cardinal directions to reduce the air-conditioning costs in the buildings. In addition, a cost analysis was performed to compute the net annual cooling and heating cost savings associated with each reflective triple glazed window unit (TWG1 to TWG60) compared to the clear triple glazing one. Results revealed the best reflective triple glazed unit to reduce cooling and heating load in both the summer and winter periods, respectively, for net air-conditioning cost savings.

- The South-East oriented TWG35 window unit (Grey reflective glass-Air Gap-Green reflective glass-Air Gap-Gold reflective glass) was the most energy-efficient among all other studied glazings with the highest net annual cost savings 16.72 $\$/m^2$.
- It was observed that all grey reflective glass window units (TWG25 to TWG36) were shown to have the highest annual cost savings, whereas all gold reflective glass window units (TWG49 to TWG60) the lowest yearly cost savings. These results indicate that the net annual cost savings depend on the reflective glass exposed to the outside environment than the reflective glass in the middle and the inside of the triple glazing unit.
- The most critical parameter for the highest air-conditioning cost savings in the triple glazing unit is the solar transmittance of the outer reflective glass. The outer reflective glass of triple glazed unit with a smaller value of solar transmittance leads to the highest air-conditioning cost savings (in $\$/m^2$). In contrast, outer reflective glass with a high solar transmittance leads to the lowest air-conditioning cost savings.
- The color rendering (Ra) and correlated color temperature (CCT) metrics of daylight through all the reflective glasses were well above the CIE recommended level, ensuring natural and vibrant daylight in building interiors.
- The TWG24 (Green reflective glass-Air gap-Bronze reflective glass-Air gap-Gold reflective glass), TWG28 (Grey reflective glass-Air gap-Gold reflective glass-Air gap-Bronze reflective glass), and TWG33 (Grey reflective glass-Air gap-Bronze reflective glass-Air gap-Gold reflective glass) window units have shown the lowest payback period of 2.1 years with annual cost savings (in $\$/m^2$) of 16, 16.26 and 16.55, respectively. TWG24, TWG28, and TWG33 units have led to the lowest payback periods despite their smaller annual cost savings than the TWG35 units (16.72 $\$/m^2$) because of their low initial implementation costs.
- The preferred order of orientation to place the triple glazing units for high net annual cost savings and the short payback period was SE < SW < S < N < NE = NW < E < W. It is not recommended to place the glazing in the east and west directions because of its insignificant annual cost savings.

Final version is available on: https://doi.org/10.1016/j.jobe.2021.103089

- Yearly net cost savings ($/m^2) of all triple glazed units were inversely proportional to their respective solar heat gain coefficients (SHGCs). The TWG35 window unit with the lowest SHGC ($SHGC_{35}$=0.14) has the highest net annual cost savings (16.72 $/m^2).
- The glazings with low operational energy have projected high net annual cost savings. It is observed that TWG 35 glazing unit had reported the lowest operational energy and the highest net annual cost savings. The TWG 34 glazing unit had reported the lowest operational energy to initial cost ratio due to low operational energy and a high initial cost.
- The sixty triple glazing window units studied reduce air-conditioning cost and give adequate average daylight factors inside the buildings.

The above-discussed results obtained from this study will be helpful in a conscious building renovation and design. Furthermore, results and insights from this research will help designers, policy-makers, and researchers to invest and further investigate the energy requirements for the well-being of the building inhabitants while considering the economic feasibility and the impact on climatic changes that the planet undergoes.

Nomenclature

TWG1	BZRGW–A–GRGW–A–GrRGW	A_G	Area of the glazing (m^2)
TWG2	BZRGW–A–GRGW–A–SPBRGW	A_1	Solar radiation in the absence of atmosphere (W/m^2)
TWG3	BZRGW–A–GRGW–A–GLDRGW	A_{SOLAR}	Solar absorbance (%)
TWG4	BZRGW–A–GrRGW–A–SPBRGW	A_o	Absorptance of the outside glass
TWG5	BZRGW–A–GrRGW–A–GLDRGW	Ac	Absorptance of the centre glass
TWG6	BZRGW–A–GrRGW–A–GRGW	Ai	Absorptance of the inside glass
TWG7	BZRGW–A–SPBRGW–A–GLDRGW	B_1	Atmospheric extinction coefficient [-]
TWG8	BZRGW–A–SPBRGW–A–GRGW	C_1	Sky radiation coefficient [-]
TWG9	BZRGW–A–SPBRGW–	C_{ag}	The thermal resistance of the air gap (m^2)

Final version is available on: https://doi.org/10.1016/j.jobe.2021.103089

	A–GrRGW		
TWG10	BZRGW–A–GLDRGW–A– GRGW	CCT	Correlated color temperature (K)
TWG11	BZRGW–A–GLDRGW–A–GrRGW	d_{ia}	Declination angle (Deg)
TWG12	BZRGW–A– GLDRGW–A–SPBRGW	t_1	The thickness of the outer glass (m)
TWG13	GRGW–A–GrRGW–A–SPBRGW	t_2	The thickness of the centre glass (m)
TWG14	GRGW–A–GrRGW–A–GLDRGW	t_3	The thickness of the inner glass (m)
TWG15	GRGW–A–GrRGW–A–BZRGW	H	Hour angle (Deg)
TWG16	GRGW–A–SPBRGW–A–GLDRGW	h_o	Outside heat transfer coefficient (W/m^{2}K)
TWG17	GRGW–A–SPBRGW–A–BZRGW	h_i	Inside heat transfer coefficient (W/m^{2}K)
TWG18	GRGW–A–SPBRGW–A–GrRGW	I_{DN}	Solar energy at normal incidence (W/m^2)
TWG19	GRGW–A–GLDRGW–A–BZRGW	I_{DSR}	Direct solar energy from the sun (W/m^2)
TWG20	GRGW–A–GLDRGW–A–GrRGW	I_{dSR}	Diffuse solar energy from the sky (W/m^2)
TWG21	GRGW–A–GLDRGW–A–SPBRGW	I_{GRD}	Ground reflected solar radiation (W/m^2)
TWG22	GRGW–A–BZRGW–A–GrRGW	I_T	Total incident solar radiation (W/m^2)
TWG23	GRGW–A–BZRGW–A–SPBRGW	I_{TRTGW}	Total heat gain through a triple glass window(W/m^2)
TWG24	GRGW–A–BZRGW–A–GLDRGW	K	Angle of window glass from vertical (Deg)
TWG25	GrRGW–A–SPBRGW–A–GLDRGW	K_1	Thermal conductivity of the outside glass (W/m K)
TWG26	GrRGW–A–SPBRGW–A–BZRGW	K_2	Thermal conductivity of the centre glass (W/m K)
TWG27	GrRGW–A–SPBRGW–	K_3	Thermal conductivity of the inside glass

	A–GRGW		(W/m K)
TWG28	GrRGW–A–GLDRGW–A–BZRGW	L	Latitude (Deg)
TWG29	GrRGW–A–GLDRGW–A–GRGW	LAT	Local apparent time
TWG30	GrRGW–A–GLDRGW–A–SPBRGW	n_d	number of days (Starts from Jan 1st)
TWG31	GrRGW–A–BZRGW–A–GRGW	q_{ds}	Daily average solar heat incident on a surface in summer (kW)
TWG32	GrRGW–A–BZRGW–A–SPBRGW	q_{dw}	Daily average solar heat incident on a surface in winter (kW)
TWG33	GrRGW–A–BZRGW–A–GLDRGW	$Q_{Sol, Sum}$	Solar radiation incident on the glass during the summer season
TWG34	GrRGW–A–GRGW–A–SPBRGW	$Q_{Sol, Win}$	Solar radiation incident on the glass during the summer season
TWG35	GrRGW–A–GRGW–A–GLDRGW	R_{SOLAR}	Solar reflectance (%)
TWG36	GrRGW–A–GRGW–A–BZRGW	Ra	General Color Rendering Index
TWG37	SPBRGW–A–GLDRGW–A–BZRGW	R_o	Reflectance of the outside glass
TWG38	SPBRGW–A–GLDRGW–A–GRGW	Rc	Reflectance of the centre glass
TWG39	SPBRGW–A–GLDRGW–A–GrRGW	Ri	Reflectance of the inside glass
TWG40	SPBRGW–A–BZRGW–A–GRGW	$SHGC_{TCWG}$	SHGC of the clear glass triple glazing
TWG41	SPBRGW–A–BZRGW–A–GrRGW	$SHGC_{TWG}$	SHGC of the reflective triple glazing
TWG42	SPBRGW–A–BZRGW–A–GLDRGW	T_o	Transmittance of the outside glass
TWG43	SPBRGW–A–GRGW–A–GrRGW	T_m	Transmittance of the centre glass
TWG44	SPBRGW–A–GRGW–A–	T_i	Transmittance of the inside glass

Final version is available on: https://doi.org/10.1016/j.jobe.2021.103089

	GLDRGW		
TWG45	SPBRGW–A–GRGW–A–BZRGW	t_{ag}	Thickness of the air space between glasses (m)
TWG46	SPBRGW–A–GrRGW–A–GLDRGW	T_{SOLAR}	Solar transmittance (%)
TWG47	SPBRGW–A–GrRGW–A–BZRGW	$T_{SOL,\ TWG}$	Solar transmittance of the reflective triple glazing (%)
TWG48	SPBRGW–A–GrRGW–A–GRGW	U_3	Unsteady transmittance of the triple glazing (W/m^2K)
TWG49	GLDRGW–A–BZRGW–A–GRGW		
TWG50	GLDRGW–A–BZRGW–A–GrRGW		
TWG51	GLDRGW–A–BZRGW–A–SPBRGW	**Greek letters**	
TWG52	GLDRGW–A–GRGW–A–GrRGW	λ	Wavelength (nm)
TWG53	GLDRGW–A–GRGW–A–SPBRGW	$\Delta\lambda$	Wavelength interval (nm)
TWG54	GLDRGW–A–GRGW–A–BZRGW	β	Solar altitude angle (Deg)
TWG55	GLDRGW–A–GrRGW–A–SPBRGW	$\beta_i(\lambda)$	Spectral reflectance of each test color, i
TWG56	GLDRGW–A–GrRGW–A–BZRGW	S_λ	Relative spectral distribution of the solar radiation(W/m^2)
TWG57	GLDRGW–A–GrRGW–A–GRGW	θ	Solar incidence angle (Deg)
TWG58	GLDRGW–A–SPBRGW–A–BZRGW	ϕ	Solar azimuth angle (Deg)
TWG59	GLDRGW–A–SPBRGW–A–GRGW	Ψ	Surface azimuth angle (Deg)
TWG60	GLDRGW–A–SPBRGW–A–GrRGW	γ	Surface solar azimuth angle (Deg)
BZRGW	Bronze reflective glass window	ρ	Glass density [kg/m^3]
GRGW	Green reflective glass	ρ_g	Ground reflectance factor [-]

	window		
SPBRGW	Sapphire blue reflective glass window	$\tau(\lambda)$	Spectral transmission (%)
GLDRGW	Gold reflective glass window	$\rho(\lambda)$	Spectral reflection (%)
GrRGW	Grey reflective glass window	$\alpha(\lambda)$	Spectral absorption (%)
W_{ag}	Width of the air space between glasses (m)	α_o	Solar absorbance of the outside glass (%)
		α_i	Solar absorbance of the inside glass (%)

References

[1] F. Asdrubali, G. Grazieschi, Life cycle assessment of energy efficient buildings, Energy Reports. 6 (2020) 270–285. https://doi.org/10.1016/j.egyr.2020.11.144.

[2] J. Mukhopadhyay, J. Ore, K. Amende, Assessing housing retrofits in historic districts in Havre Montana, Energy Reports. 5 (2019) 489–500. https://doi.org/10.1016/j.egyr.2019.03.008.

[3] J. Avila-Delgado, MD. Robador, J.A. Barrera-Vera, M. Marrero, Glazing selection procedure for office building retrofitting in the Mediterranean climate in Spain, J. Build. Eng. 33 (2021). https://doi.org/10.1016/j.jobe.2020.101448

[4] M. Mustafa, S. Ali, J.R. Snape, B. Vand, Investigations towards lower cooling load in a typical residential building in Kurdistan (Iraq), Energy Reports. 6 (2020) 571–580. https://doi.org/10.1016/j.egyr.2020.11.011.

[5] E. Cuce, Accurate and reliable U-value assessment of argon-filled double glazed windows: A numerical and experimental investigation, Energy Build. 171 (2018) 100–106. https://doi.org/10.1016/j.enbuild.2018.04.036.

[6] Y. Fang, T.J. Hyde, F. Arya, N. Hewitt, R. Wang, Y. Dai, Enhancing the thermal performance of triple vacuum glazing with low-emittance coatings, Energy Build. 97 (2015) 186–195. https://doi.org/10.1016/j.enbuild.2015.04.006.

[7] B. Durakovic, S. Mesetovic, Thermal performances of glazed energy storage systems with various storage materials: An experimental study, Sustain. Cities Soc. 45 (2019) 422–430. https://doi.org/10.1016/j.scs.2018.12.003.

[8] C. Liu, Y. Wu, D. Li, Y. Zhou, Z. Wang, X. Liu, Effect of PCM thickness and melting temperature on thermal performance of double glazing units, J. Build. Eng. 11 (2017) 87–95. https://doi.org/10.1016/j.jobe.2017.04.005.

[9] F. Tang, J. Chen, J. Li, D. Rodriguez, Energy saving actions toward NZEBs with multiple-criteria optimization in current residential buildings, Energy Reports. 6 (2020) 3008–3022. https://doi.org/10.1016/j.egyr.2020.10.069.

[10] Y. Zhou, S. Zheng, Machine learning-based multi-objective optimisation of an aerogel glazing system using NSGA-II—study of modelling and application in the subtropical climate Hong Kong, J. Clean. Prod. 253 (2020) 119964. https://doi.org/10.1016/j.jclepro.2020.119964.

[11] K.K. Gorantla, S. Shaik, A.B.T. Puttaranga Setty, Simulation of various wall and window glass material for energy efficient building design, Key Eng. Mater. 692 (2016) 9–16. https://doi.org/10.4028/www.scientific.net/KEM.692.9.

[12] T. Ashrafian, N. Moazzen, The impact of glazing ratio and window configuration on occupants' comfort and energy demand: The case study of a school building in Eskisehir, Turkey, Sustain. Cities Soc. 47 (2019) 101483. https://doi.org/10.1016/j.scs.2019.101483.

[13] S. Pal, B. Roy, S. Neogi, Heat transfer modelling on windows and glazing under the exposure of solar radiation, Energy Build. 41 (2009) 654–661. https://doi.org/10.1016/j.enbuild.2009.01.003.

[14] C. Lee, J. Won, Analysis of combinations of glazing properties to improve economic efficiency of buildings, J. Clean. Prod. 166 (2017) 181–188. https://doi.org/10.1016/j.jclepro.2017.08.024.

[15] A.R. Amaral, E. Rodrigues, A.R. Gaspar, Á. Gomes, A thermal performance parametric study of window type, orientation, size and shadowing effect, Sustain. Cities Soc. 26 (2016) 456–465. https://doi.org/10.1016/j.scs.2016.05.014.

[16] W.J. Hee, M.A. Alghoul, B. Bakhtyar, O. Elayeb, M.A. Shameri, M.S. Alrubaih, K. Sopian, The role of window glazing on daylighting and energy saving in buildings, Renew. Sustain. Energy Rev. 42 (2015) 323–343. https://doi.org/10.1016/j.rser.2014.09.020.

[17] S. Nundy, A. Mesloub, B.M. Alsolami, A. Ghosh, Electrically actuated visible and near-infrared regulating switchable smart window for energy positive building: A review, J. Clean. Prod. 301 (2021) 126854. https://doi.org/10.1016/j.jclepro.2021.126854.

[18] S. Nundy, A. Ghosh, Thermal and visual comfort analysis of adaptive vacuum integrated switchable suspended particle device window for temperate climate, Renew. Energy. 156 (2020) 1361–1372. https://doi.org/10.1016/j.renene.2019.12.004.

[19] S. Shaik, K. Gorantla, M. Venkata Ramana, S. Mishra, K.S. Kulkarni, Thermal and cost assessment of various polymer-dispersed liquid crystal film smart windows for energy efficient buildings, Constr. Build. Mater. 263 (2020) 120155. https://doi.org/10.1016/j.conbuildmat.2020.120155.

[20] F. Isaia, M. Fiorentini, V. Serra, A. Capozzoli, Enhancing energy efficiency and comfort in buildings through model predictive control for dynamic façades with electrochromic glazing, J. Build. Eng. 43 (2021) 102535. https://doi.org/10.1016/j.jobe.2021.102535.

[21] B.P. Jelle, Solar radiation glazing factors for window panes, glass structures and electrochromic windows in buildings - Measurement and calculation, Sol. Energy Mater. Sol. Cells. 116 (2013) 291–323. https://doi.org/10.1016/j.solmat.2013.04.032.

[22] A. Ghosh, B. Norton, Optimization of PV powered SPD switchable glazing to minimise probability of loss of power supply, Renew. Energy. 131 (2019) 993–1001. https://doi.org/10.1016/j.renene.2018.07.115.

[23] C. Garlisi, E. Trepci, R. Al Sakkaf, E. Azar, G. Palmisano, Combining energy efficiency with self-cleaning properties in smart glass functionalized with multilayered semiconductors, J. Clean. Prod. (2020) 122830. https://doi.org/10.1016/j.jclepro.2020.122830.

[24] A. Ghosh, B. Norton, T.K. Mallick, Influence of atmospheric clearness on PDLC switchable glazing transmission, Energy Build. 172 (2018) 257–264. https://doi.org/10.1016/j.enbuild.2018.05.008.

[25] A. Ghosh, B. Norton, A. Duffy, Effect of sky conditions on light transmission through a suspended particle device switchable glazing, Sol. Energy Mater. Sol. Cells. 160 (2017) 134–140. https://doi.org/10.1016/j.solmat.2016.09.049.

[26] A. Ghosh, B. Norton, A. Duffy, Effect of atmospheric transmittance on performance of adaptive SPD-vacuum switchable glazing, Sol. Energy Mater. Sol. Cells. 161 (2017) 424–431. https://doi.org/10.1016/j.solmat.2016.12.022.

[27] A. Sharda, S. Kumar, Comparative study of simulation and experimentation for the u-value of double-glazed windows with inter-pane blinds, Sci. Technol. Built Environ. 21 (2015) 179–189. https://doi.org/10.1080/10789669.2014.985965.

[28] Y. Sun, Y. Wu, R. Wilson, S. Lu, Experimental measurement and numerical simulation of the thermal performance of a double glazing system with an interstitial Venetian blind, Build. Environ. 103 (2016) 111–122. https://doi.org/10.1016/j.buildenv.2016.03.028.

[29] H.M. Taleb, A.G. Antony, Assessing different glazing to achieve better lighting performance of office buildings in the United Arab Emirates (UAE), J. Build. Eng. 28 (2020) 101034. https://doi.org/10.1016/j.jobe.2019.101034.

[30] A. Dutta, A. Samanta, Reducing cooling load of buildings in the tropical climate through window glazing: A model to model comparison, J. Build. Eng. 15 (2018) 318–327. https://doi.org/10.1016/j.jobe.2017.12.005.

[31] D.G. Zenginis, K.J. Kontoleon, Influence of orientation, glazing proportion and zone aspect ratio on the thermal performance of buildings during the winter period, Environ. Sci. Pollut. Res. 25 (2018) 26736–26746. https://doi.org/10.1007/s11356-017-9700-3.

[32] S. Jaber, S. Ajib, Thermal and economic windows design for different climate zones, Energy Build. 43 (2011) 3208–3215. https://doi.org/10.1016/j.enbuild.2011.08.019.

[33] P. Ihm, L. Park, M. Krarti, D. Seo, Impact of window selection on the energy performance of residential buildings in South Korea, Energy Policy. 44 (2012) 1–9. https://doi.org/10.1016/j.enpol.2011.08.046.

[34] J.S. Carlos, H. Corvacho, Evaluation of the performance indices of a ventilated double window through experimental and analytical procedures: SHGC-values, Energy Build. 86 (2015) 886–897. https://doi.org/10.1016/j.enbuild.2014.11.002.

[35] K. Gorantla, S. Shaik, A.B.T.P. Setty, Effect of Different Double Glazing Window Combinations on Heat gain in Buildings for Passive Cooling in Various Climatic Regions of India, Mater. Today Proc. 4 (2017) 1910–1916. https://doi.org/10.1016/j.matpr.2017.02.036.

[36] K.K. Gorantla, S. Shaik, A.B.T.P.R. Setty, Day lighting and thermal analysis using various double reflective window glasses for green energy buildings, Int. J. Heat Technol. 36 (2018) 1121–1129. https://doi.org/10.18280/ijht.360345.

[37] G. Kirankumar, S. Saboor, S.S. Vali, D. Mahapatra, A.B. Talanki Puttaranga Setty, K.H. Kim, Thermal and cost analysis of various air filled double glazed reflective windows for energy efficient buildings, J. Build. Eng. 28 (2020) 101055. https://doi.org/10.1016/j.jobe.2019.101055.

[38] K. Gorantla, S. Shaik, A.B.T.P.R. Setty, Thermal and energy saving analysis by using tinted double window glass combinations for heat gain in buildings, Int. Energy J. 18 (2018) 215–230.

[39] K.J. Kontoleon, Glazing solar heat gain analysis and optimization at varying orientations and placements in aspect of distributed radiation at the interior surfaces, Appl. Energy. 144 (2015) 152–164. https://doi.org/10.1016/j.apenergy.2015.01.087.

[40] ASTM E 424-71, Test for solar energy transmittance and reflectance of sheet materials, Am. Soc. Test. Mater. (2015).

[41] BS EN 410, Glass in building - Determination of luminous and solar characteristics of glazing, British Standards Institution (2011).

[42] ISO 9050, Glass in buildings-Determination of light tranmisttance, solar direct transmittance, and related glazing factors, (2003).

[43] R. Dangol, T. Kruisselbrink, A. Rosemann, Effect of window glazing on colour quality of transmitted daylight, J. Daylighting. 4 (2017) 37–47. https://doi.org/10.15627/jd.2017.6.

[44] A. Ghosh, B. Norton, Interior colour rendering of daylight transmitted through a suspended particle device switchable glazing, Sol. Energy Mater. Sol. Cells. 163

(2017) 218–223. https://doi.org/10.1016/j.solmat.2017.01.041.

[45] CIBSE, CIBSE Environmental Design Guide-A, The Chartered Institution of Building Services Engineers, London (U.K.), (2006).

[46] ECBC, Energy Conservation Building Code. Bureau of Energy Efficiency, New Delhi, (2017).

[47] A. Mani, Solar Radiation Hand BookSolar radiation over India, Allied Publ. Priv. Limited, India. (1982) 1986–2000.

[48] SP 41, Handbook on Functional Requirements of Buildings (Other than Industrial Buildings), Bur. Indian Stand. India. 33–40 (1987).

[49] NBC, National Building Code of India, BIS , New Delhi, India. 112 (2005) 211–212.

[50] J.A. Duffie, W.A. Beckman, J. McGowan, Solar Engineering of Thermal Processes, (1985).

[51] G.V. Parishwad, R.K. Bhardwaj, V.K. Nema, A Theoretical Procedure for Estimation of Solar Heat Gain Factor for India, Archit. Sci. Rev. 41 (1998) 11–15. https://doi.org/10.1080/00038628.1998.9697402.

[52] ASHRAE, ASHRAE Handbook of Fundamentals, Ashrae Standard (2001).

[53] Y.A. Cengel, Heat Transfer, Tata McGraw Hill Publications. U.K. (2010).

[54] K.K. Gorantla, S. Saboor, V. Kumar, K.H. Kim, A.B.T. P. Setty, Experimental and theoretical studies of various solar control window glasses for the reduction of cooling and heating loads in buildings across different climatic regions, Energy Build. 173 (2018) 326–336. https://doi.org/10.1016/j.enbuild.2018.05.054.

LIST OF FIGURES:

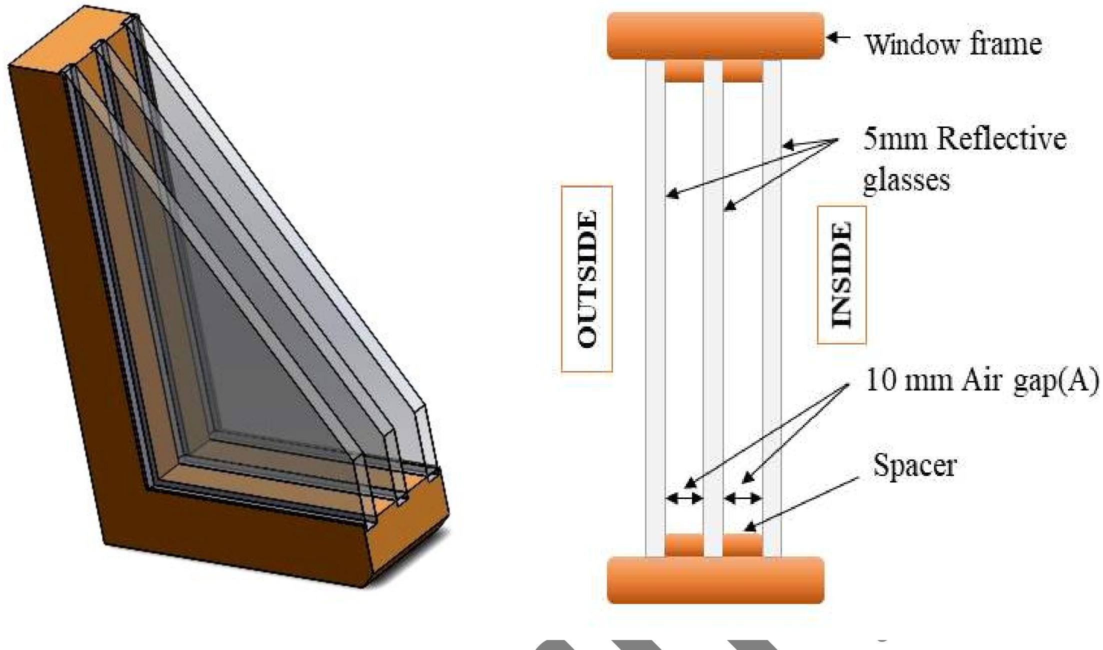

3D view of glazing system **Cross Section of glazing system**

Fig. 1. Outline of a triple glazed unit consisting of reflective glasses

Final version is available on: https://doi.org/10.1016/j.jobe.2021.103089

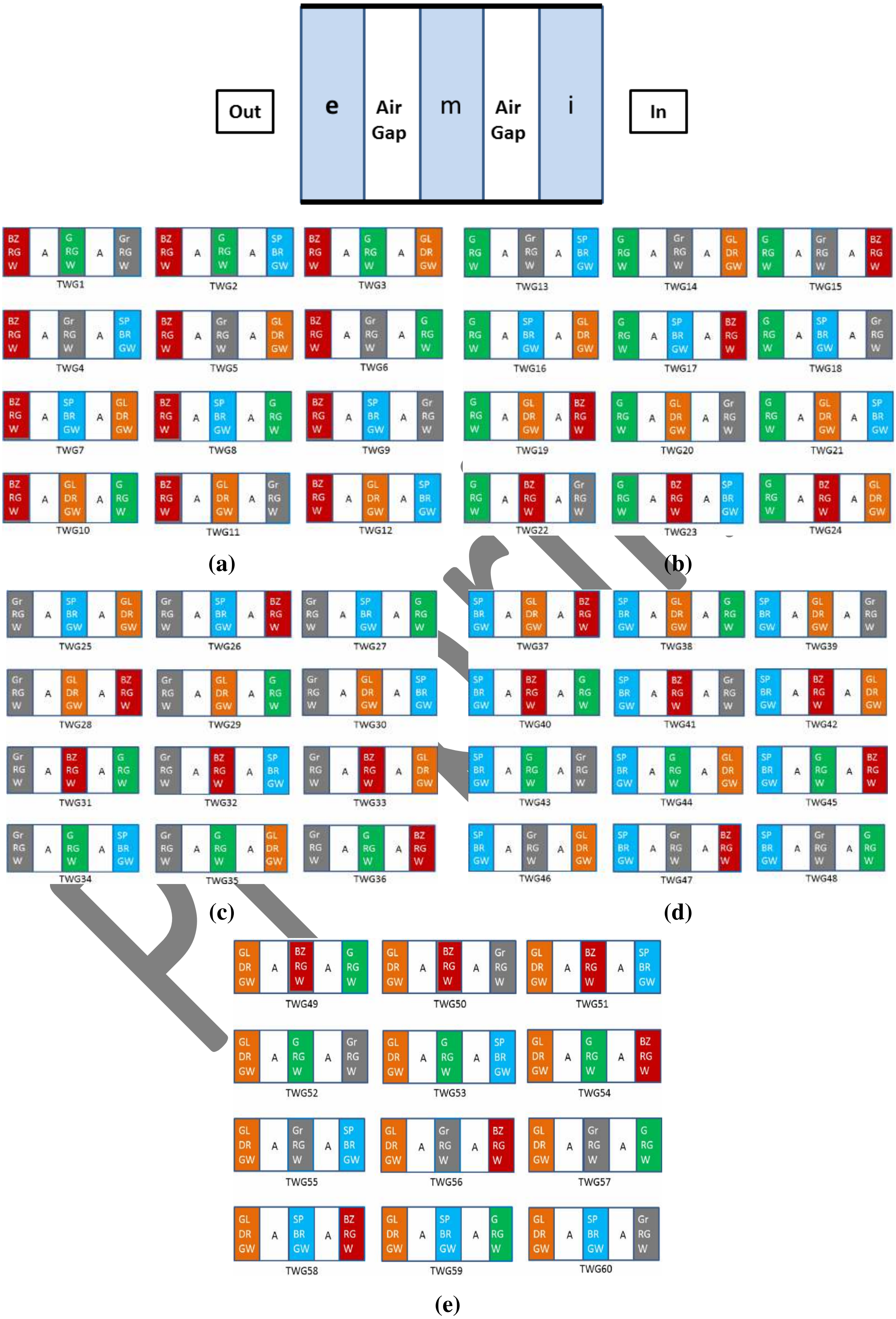

Final version is available on: https://doi.org/10.1016/j.jobe.2021.103089

Fig. 2. Reflective triple glazing configurations with: (a) Bronze color; (b) Green color; (c) Grey color; (d) Sapphire blue color; (e) Gold color

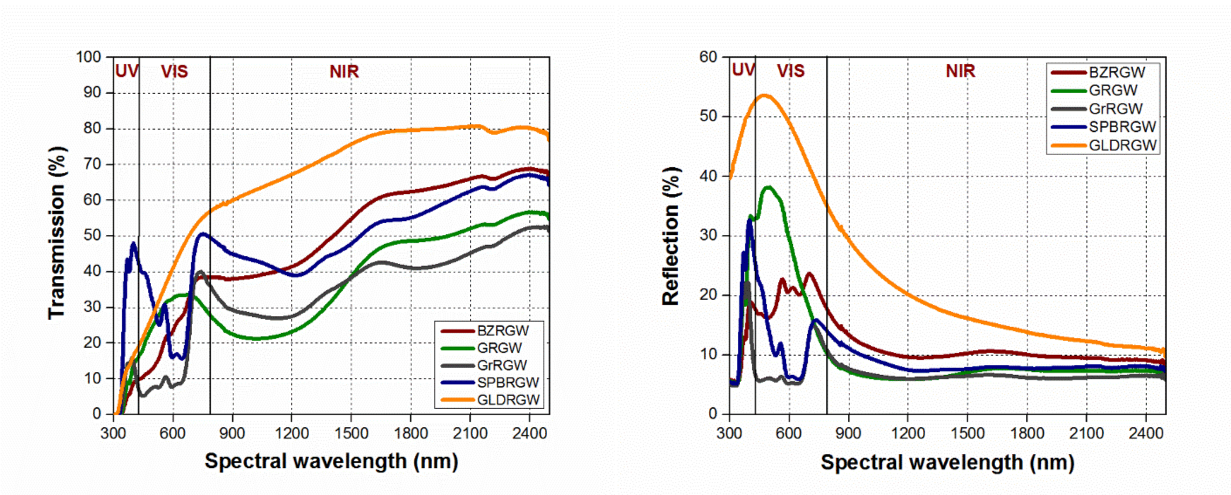

(a) Transmission (%T)

(b) Reflection (%R)

Fig. 3. Spectral characteristics of reflective glasses.

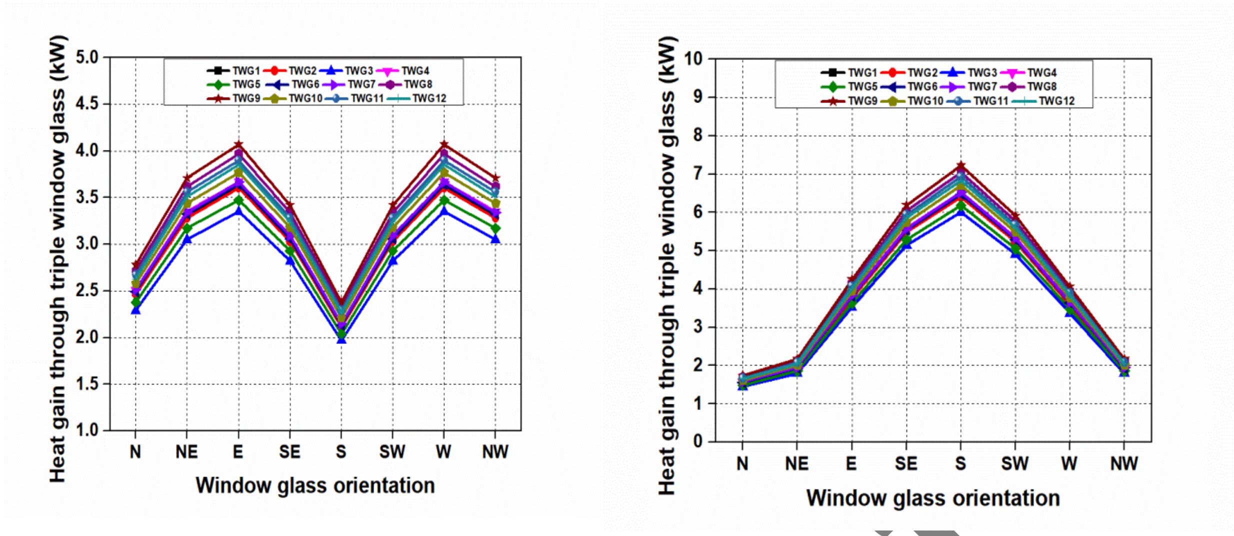

(a) Peak Summer

(b) Peak Winter

Fig. 4. Solar heat gain through triple bronze reflective glass window units.

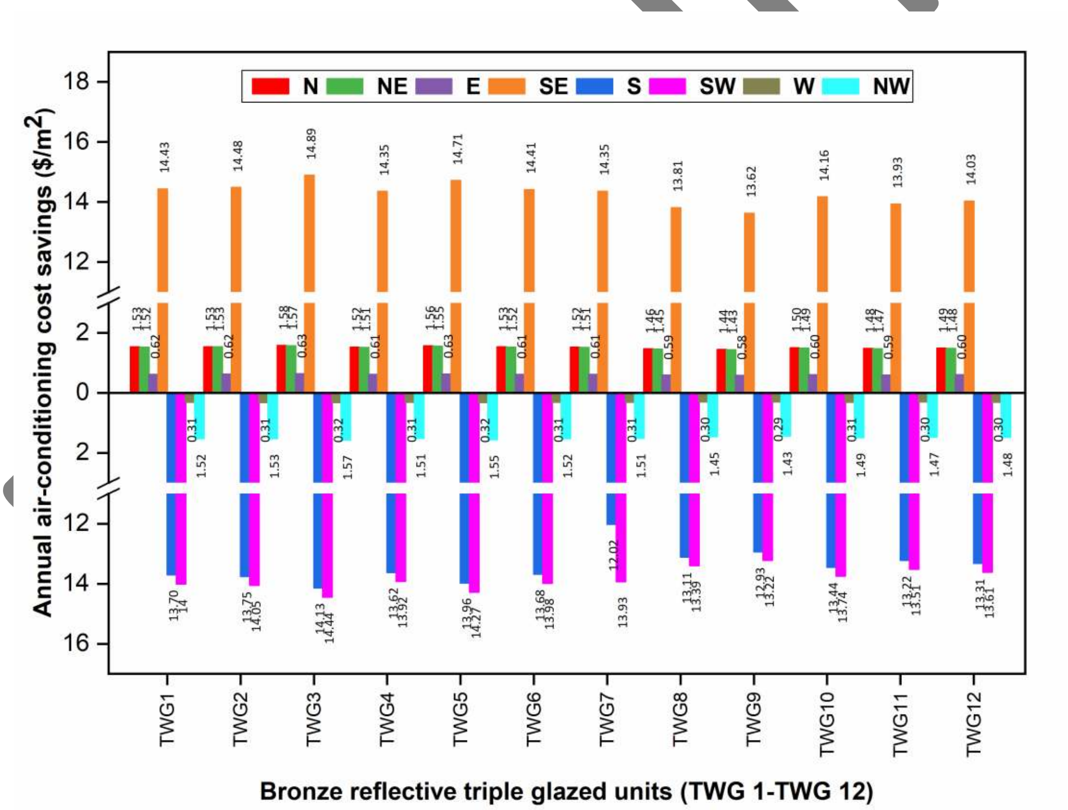

Fig. 5. Annual air-conditioning cost savings of triple bronze reflective glass window units in all orientations

Final version is available on: https://doi.org/10.1016/j.jobe.2021.103089

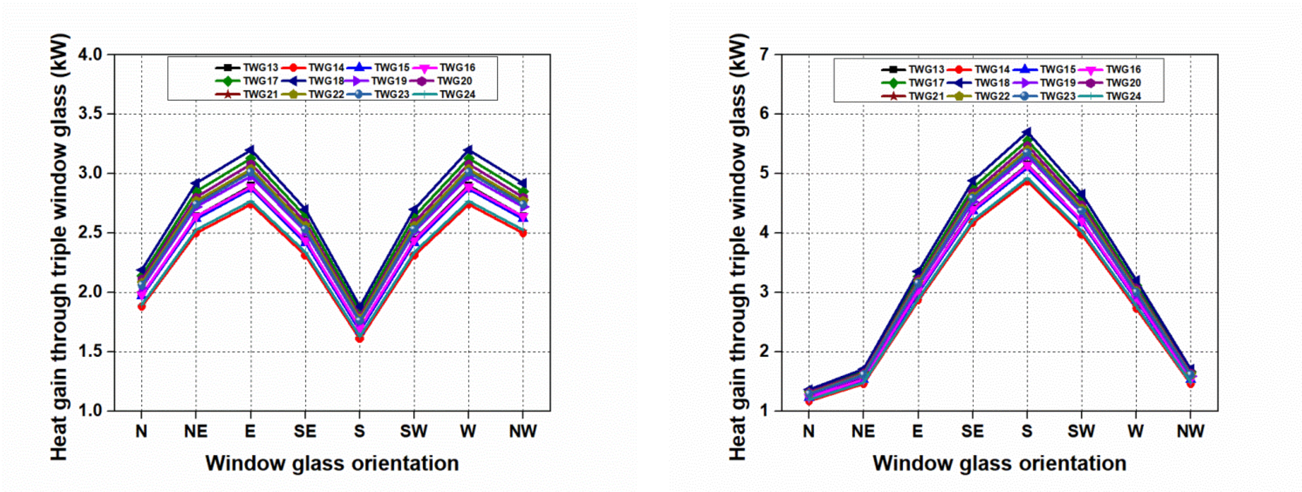

(a) Peak Summer (b) Peak Winter

Fig. 6. Total heat gains (kW) through triple green reflective glass window units in buildings in all orientations (a) Peak summer (b) Peak winter

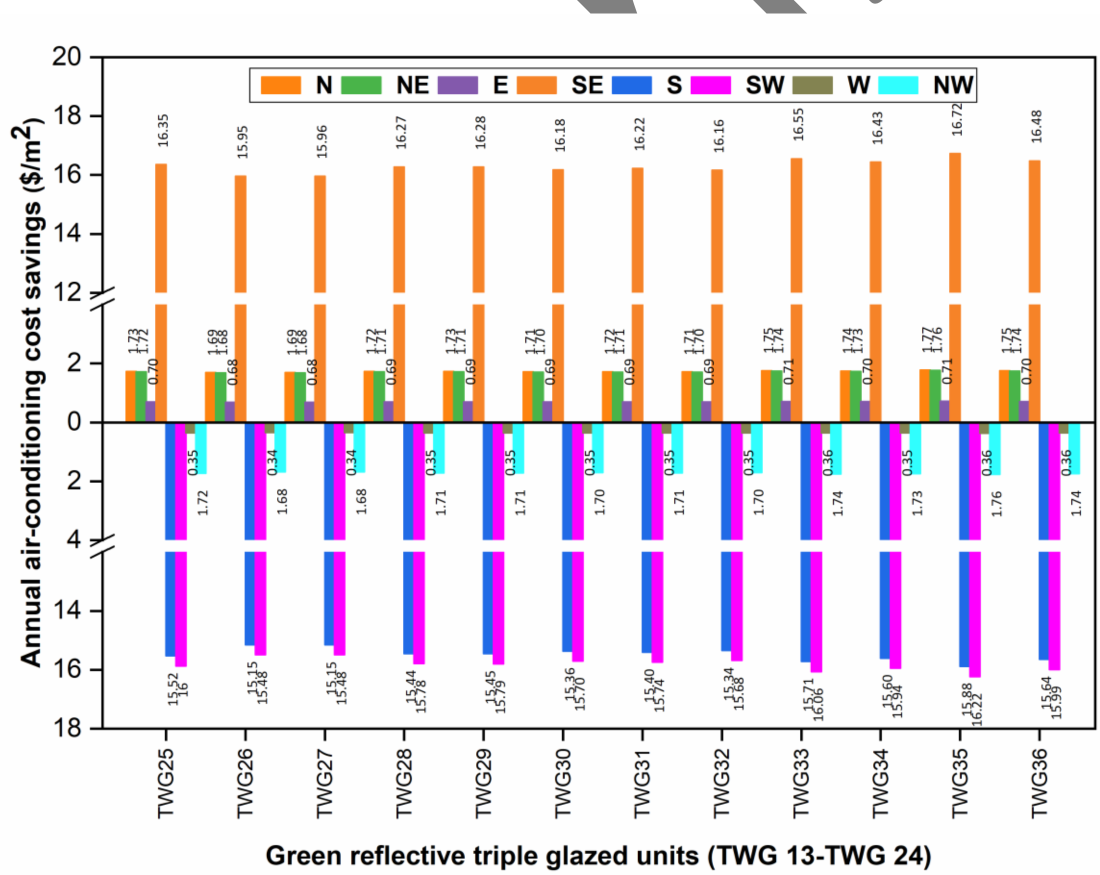

Fig. 7. Annual air-conditioning cost savings of triple green-reflective glass window units in all orientations

Final version is available on: https://doi.org/10.1016/j.jobe.2021.103089

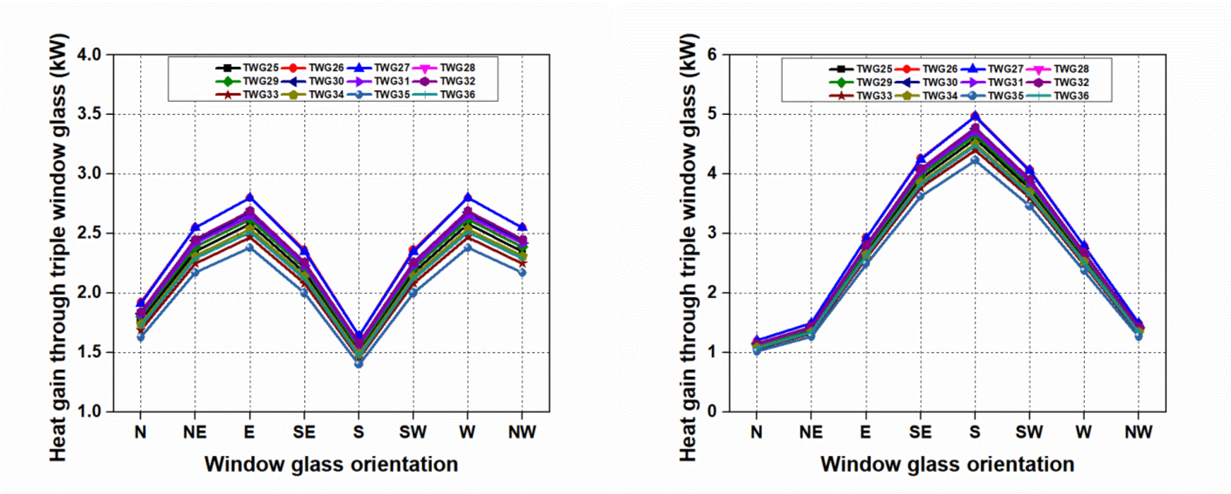

(a) (b)

Fig. 8. Total heat gains through triple grey reflective window glass units in buildings in all orientations during (a) Peak summer (b) Peak winter

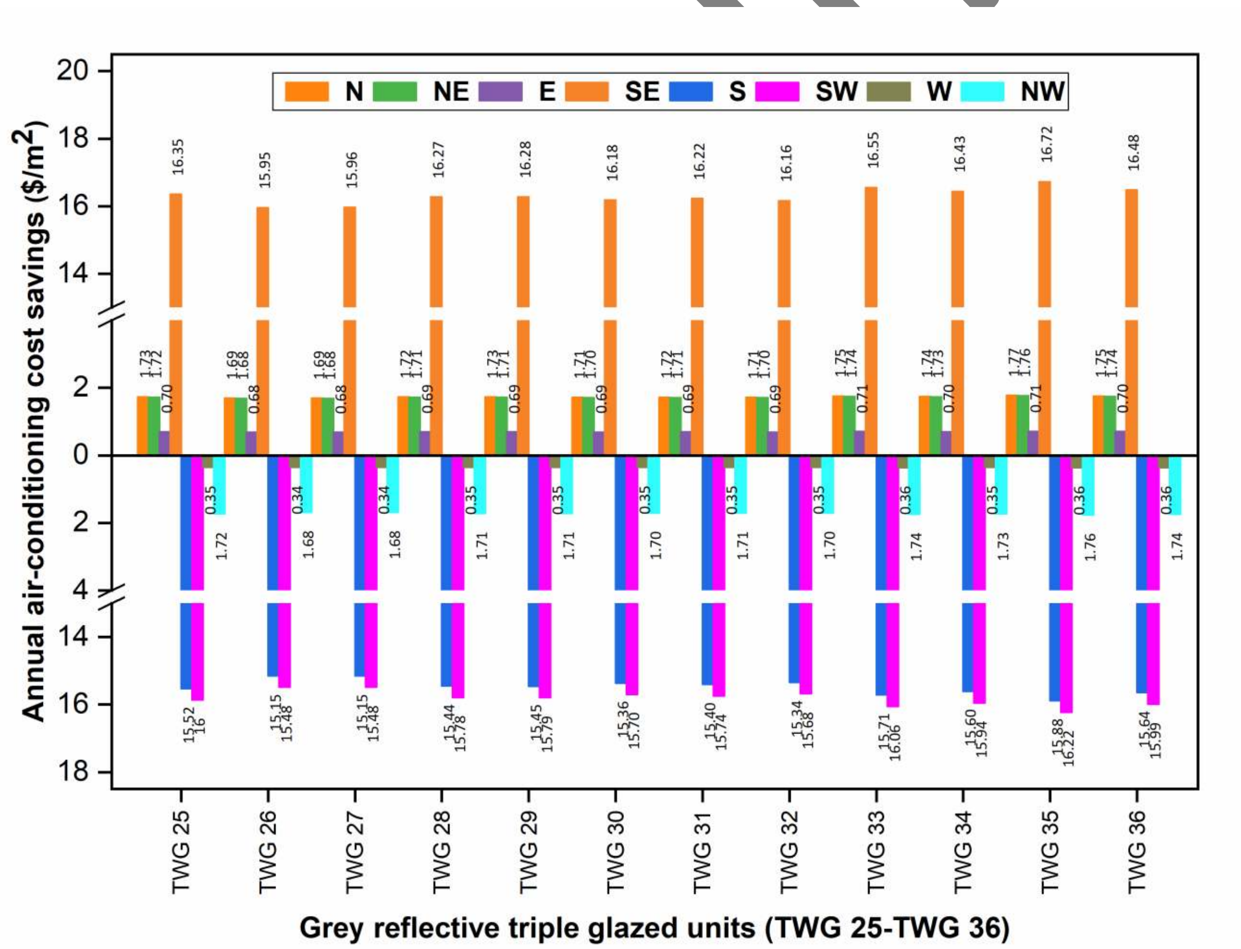

Fig. 9. Annual air-conditioning cost savings ($/m^2) of triple grey reflective glass window units in all orientations

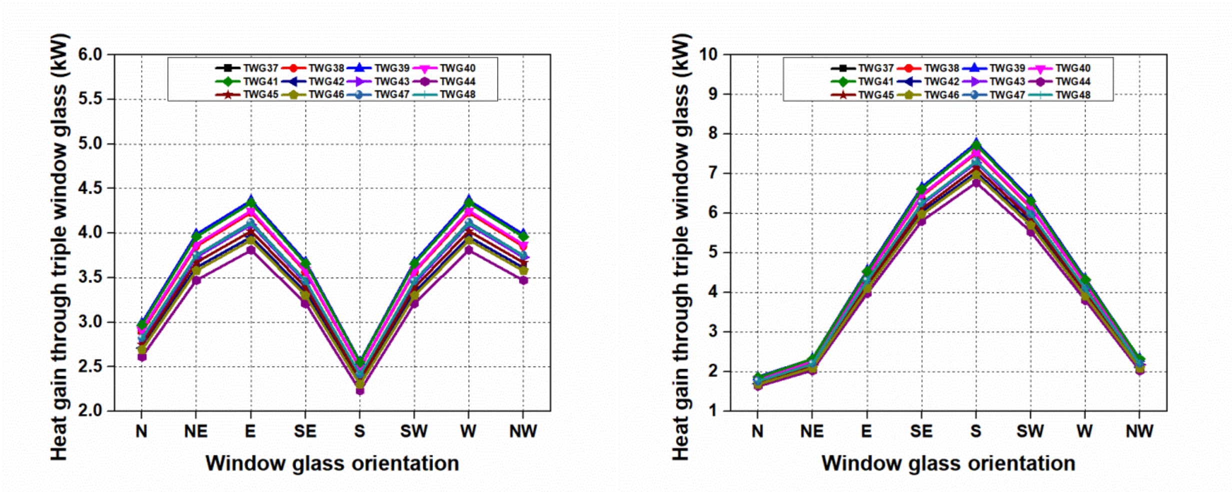

(a) Peak Summer (b) Peak Winter

Fig. 10. Total heat gains through triple sapphire blue reflective window glass units in buildings (a) Summer (b) Winter

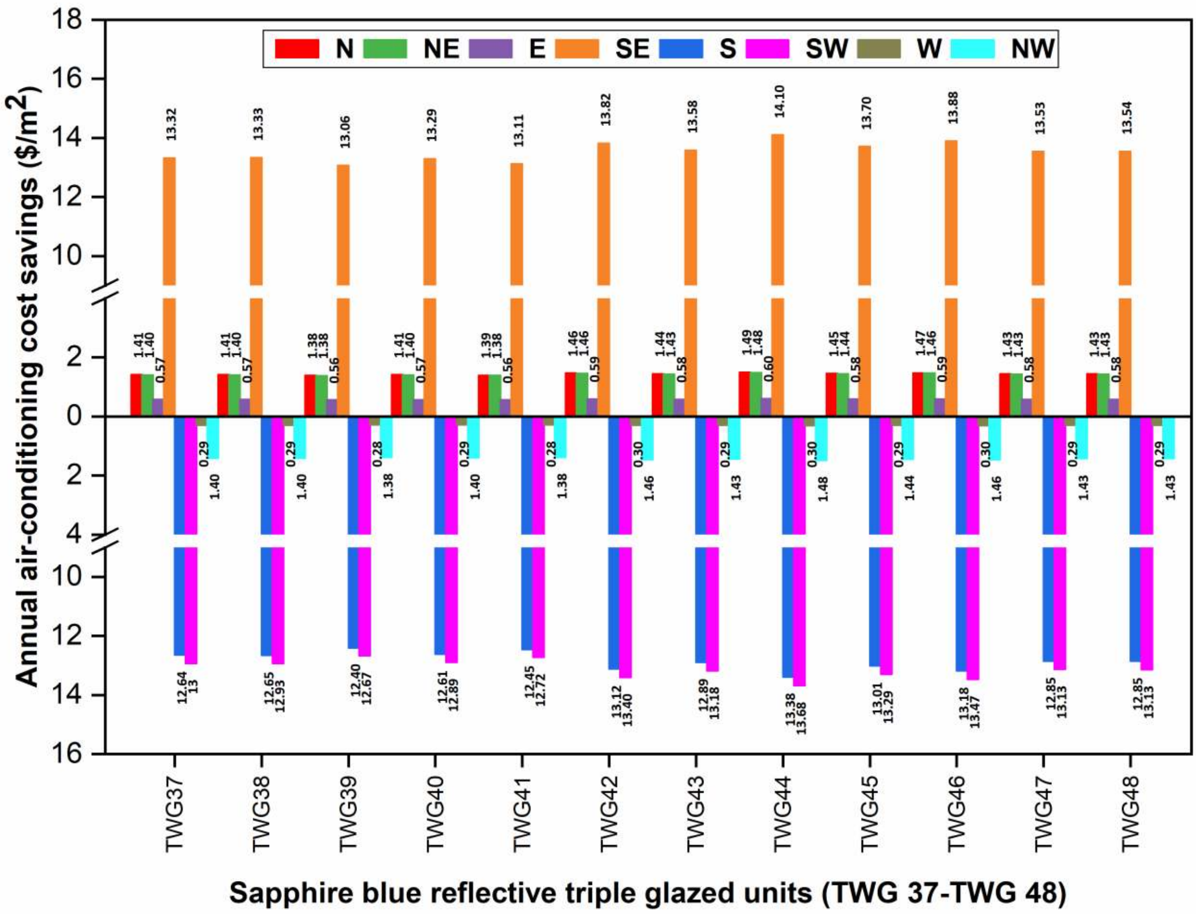

Fig. 11. Annual air-conditioning cost savings of triple sapphire blue-reflective window units in all orientations

Final version is available on: https://doi.org/10.1016/j.jobe.2021.103089

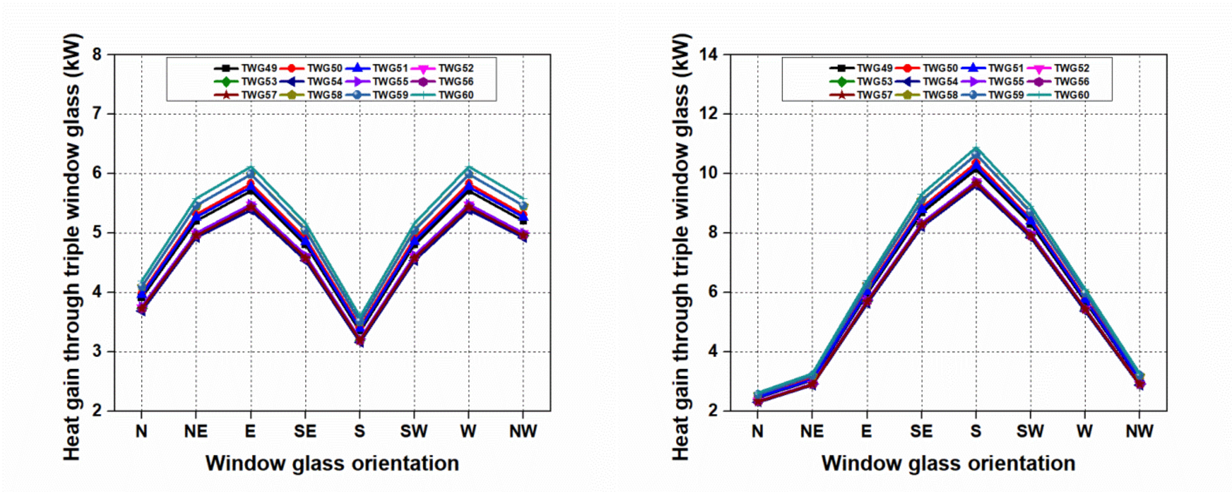

(a) Peak Summer (b) Peak Winter

Fig. 12. Solar heat gains (kW) through the triple gold reflective glass window in buildings in all orientations

(a) Peak summer (b) Peak winter

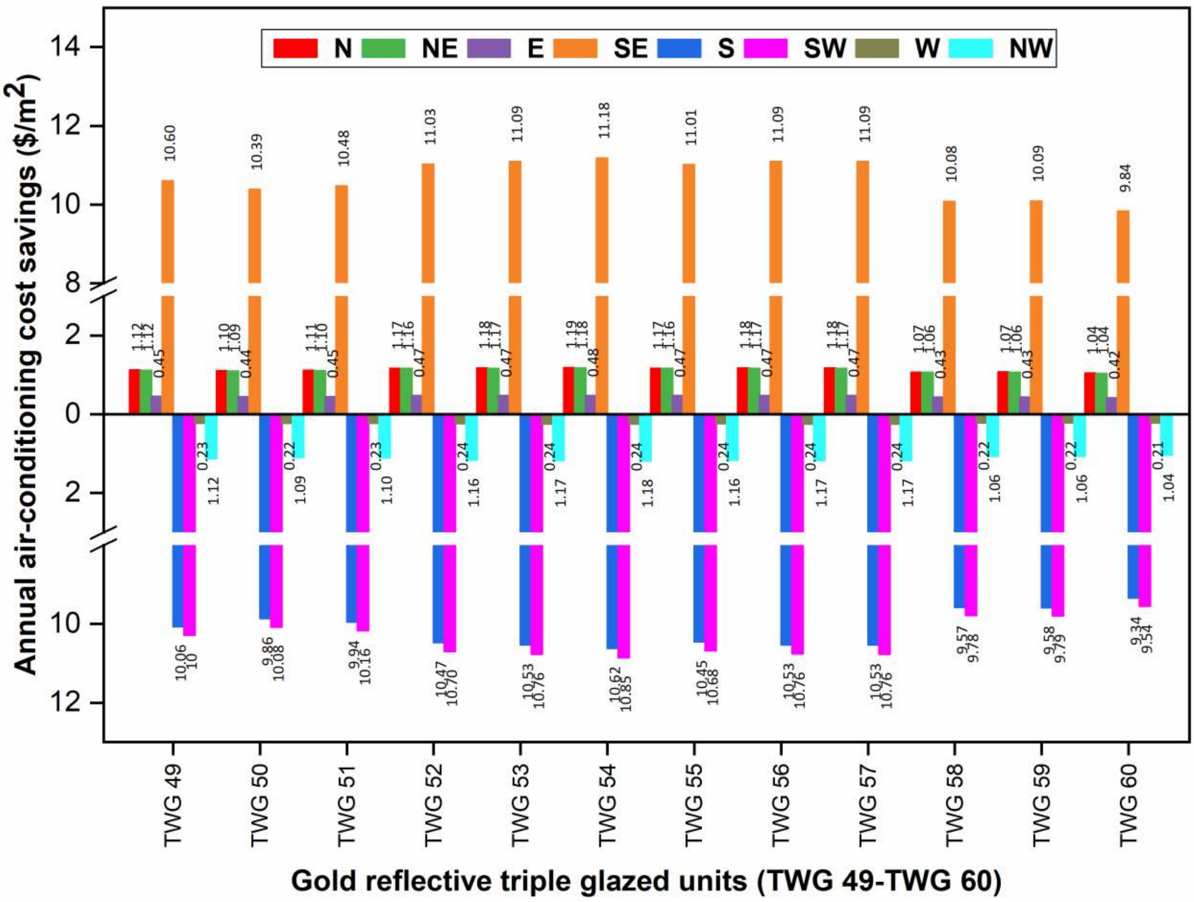

Fig. 13. Annual air-conditioning cost savings of triple gold reflective glass window units in all orientations

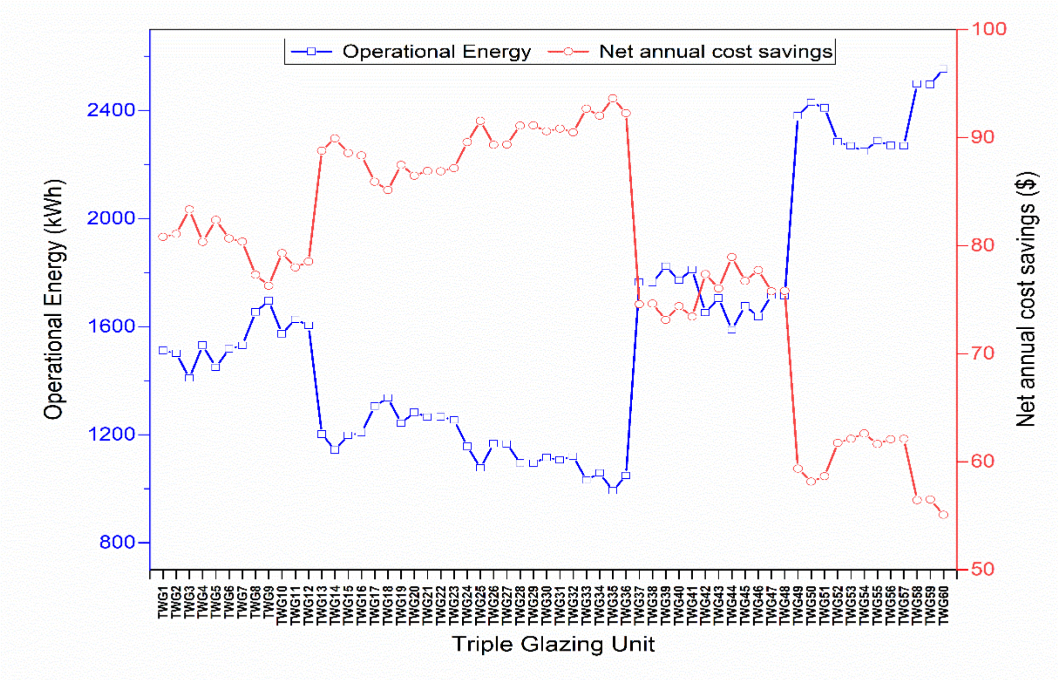

Fig. 14. Operational energy and Net annual cost savings of triple glazing units in S-E orientation

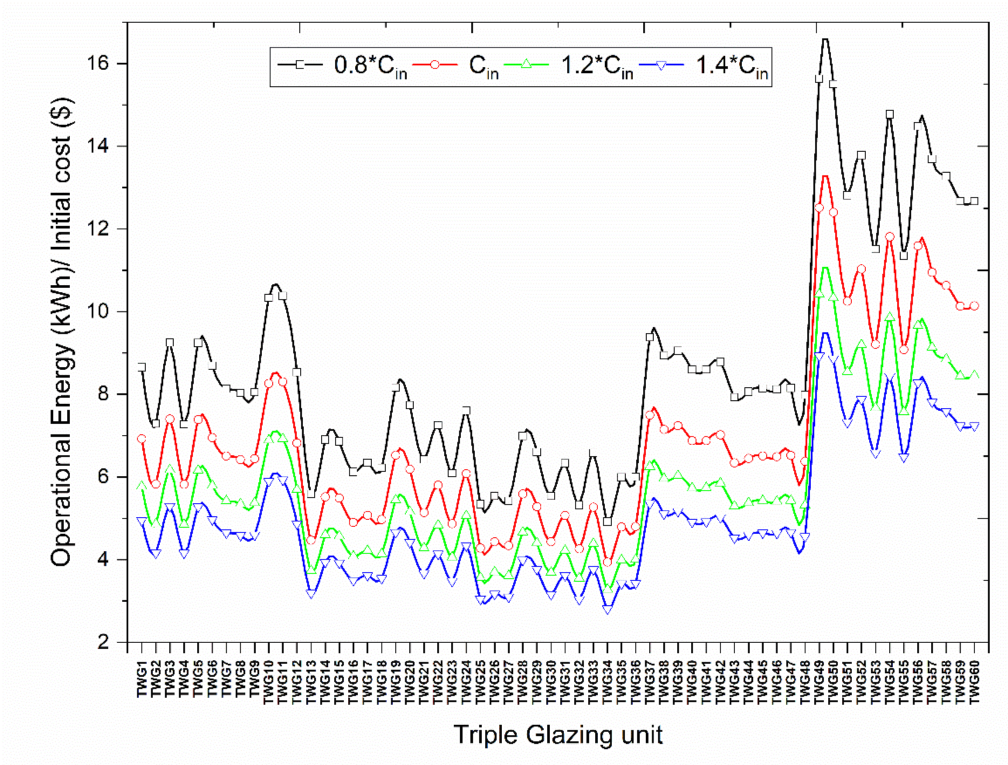

Fig. 15. Operational energy and initial cost ratios of triple glazing units in S-E orientation

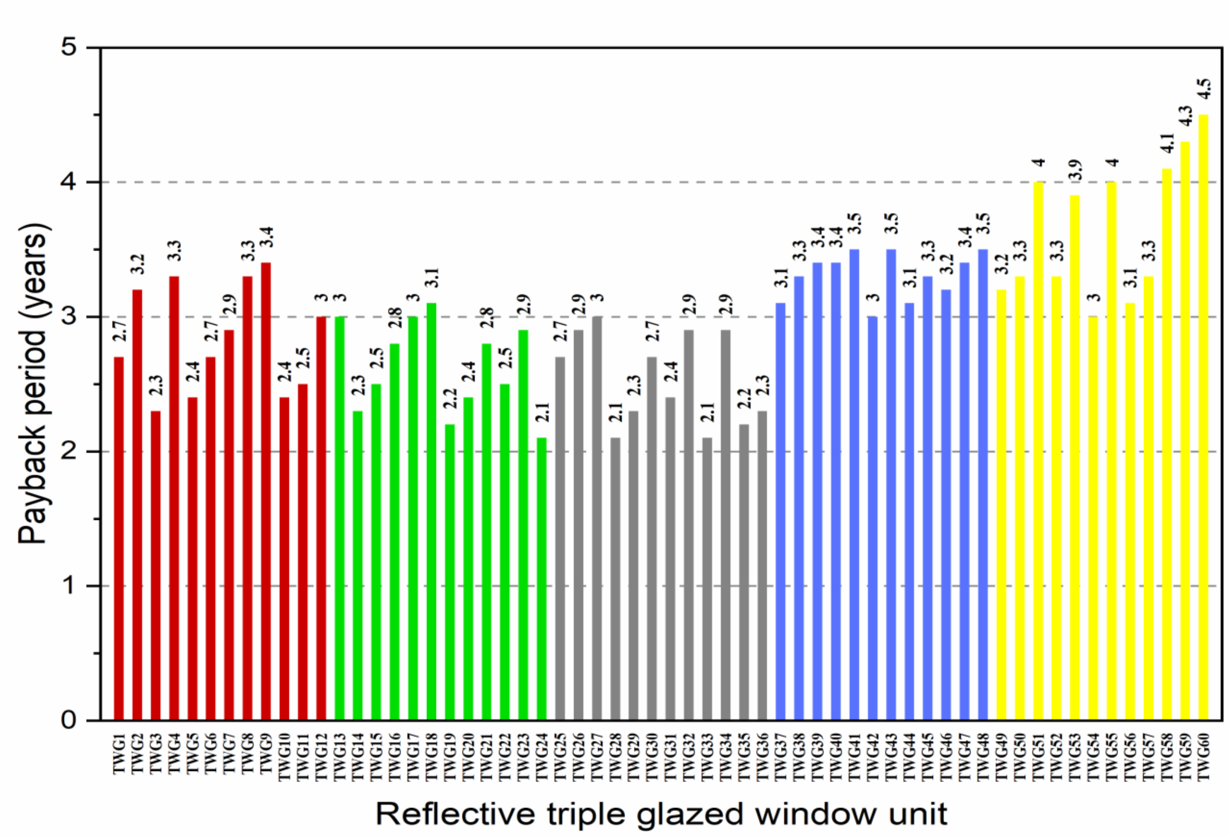

Fig. 16. The payback period for triple glazed reflective window units (TWG1 to TWG60) in the S-E orientation

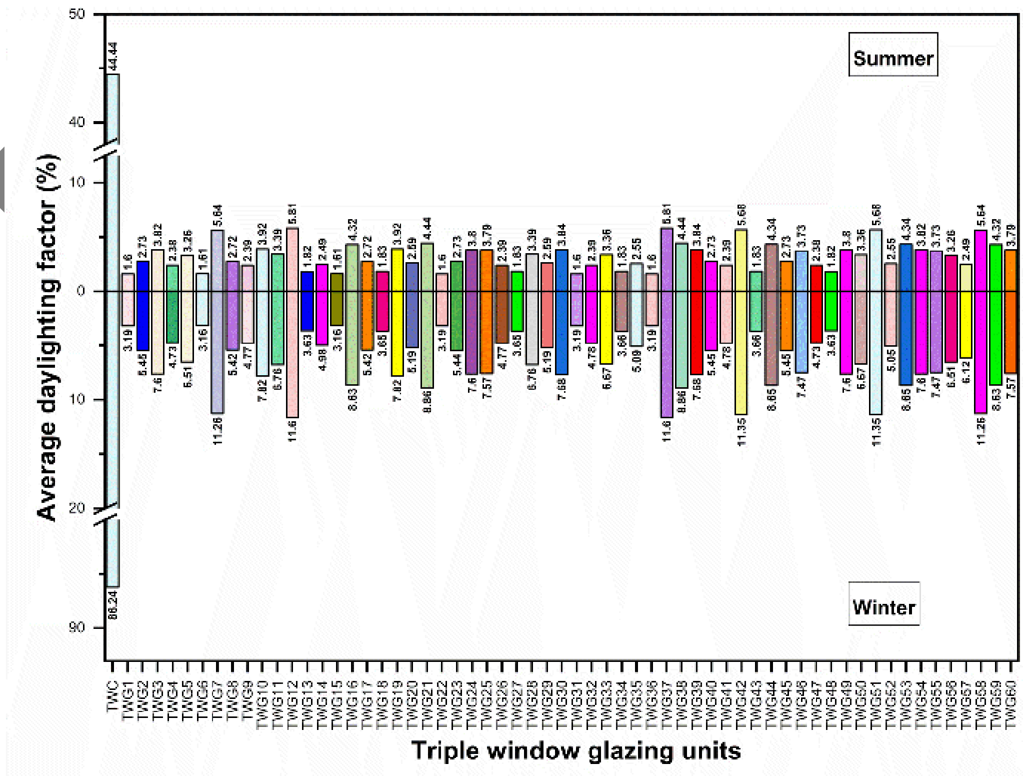

Fig. 17. Average daylight factor of triple window glazing units in S-E orientation

Final version is available on: https://doi.org/10.1016/j.jobe.2021.103089

LIST OF TABLES:

Table 1

Solar, color rendering properties and thermal indices of reflective glasses

Glass	Code	Transmittance T_{SOLAR} (%)	Reflectance R_{SOLAR} (%)	Absorbance A_{SOLAR} (%)	SHGC (%)	R_a (-)	CCT (K)
Bronze reflective glass	BZRGW	37	14	49	48	80.18	5375
Green reflective glass	GRGW	29	14	57	42	91.67	5149
Grey reflective glass	GrRGW	26	08	66	41	93.42	5114
Sapphire blue reflective glass	SPBRGW	42	11	47	53	85.54	5104
Gold reflective glass	GLDRGW	55	32	13	58	84.55	5226

Table 2

Solar heat gain coefficients (SHGCs) of all reflective triple glazed window units (TWG1 to TWG 60).

Glass unit	SHGC	Glass unit	SHGC	Glass unit	SHGC
TWG1	0.21	TWG21	0.18	TWG41	0.25
TWG2	0.21	TWG22	0.18	TWG42	0.23
TWG3	0.20	TWG23	0.18	TWG43	0.24
TWG4	0.22	TWG24	0.16	TWG44	0.22
TWG5	0.20	TWG25	0.15	TWG45	0.23
TWG6	0.21	TWG26	0.16	TWG46	0.23
TWG7	0.21	TWG27	0.16	TWG47	0.24
TWG8	0.23	TWG28	0.15	TWG48	0.24
TWG9	0.24	TWG29	0.15	TWG49	0.33
TWG10	0.22	TWG30	0.16	TWG50	0.34
TWG11	0.23	TWG31	0.16	TWG51	0.34
TWG12	0.23	TWG32	0.16	TWG52	0.32
TWG13	0.17	TWG33	0.14	TWG53	0.32
TWG14	0.16	TWG34	0.15	TWG54	0.32
TWG15	0.17	TWG35	0.14	TWG55	0.32
TWG16	0.17	TWG36	0.15	TWG56	0.32

Final version is available on: https://doi.org/10.1016/j.jobe.2021.103089

TWG17	0.18	TWG37	0.25	TWG57	0.32
TWG18	0.19	TWG38	0.25	TWG58	0.35
TWG19	0.17	TWG39	0.26	TWG59	0.35
TWG20	0.18	TWG40	0.25	TWG60	0.36

Table 3

Surface azimuths (0^o to $\pm 180^0$) for different orientations taken from the south [52]

Direction	**N**	**NE**	**E**	**SE**	**S**	**SW**	**W**	**NW**
Surface azimuth (Ψ)	-180^0	-135^0	-90^0	-45^0	$\pm 0^0$	$+45^0$	$+90^0$	$+135^0$

Table 4

Implementation and cost savings of various triple-glazed reflective glass window units in the S-E orientation

Glazing unit	**Glazing price($/m^2)**	**Annual cost savings ($/m^2)**	**Glazing unit**	**Glazing price($/m^2)**	**Annual cost savings ($/m^2)**
TWG1	39	14.43	TWG31	39	16.21
TWG2	46	14.48	TWG32	47	16.16
TWG3	34	14.89	TWG33	35	16.55
TWG4	47	14.36	TWG34	48	16.43
TWG5	35	14.71	TWG35	37	16.71
TWG6	39	14.41	TWG36	39	16.48
TWG7	42	14.36	TWG37	42	13.32
TWG8	46	13.80	TWG38	44	13.32
TWG9	47	13.63	TWG39	45	13.05
TWG10	34	14.16	TWG40	46	13.29
TWG11	35	13.91	TWG41	47	13.11
TWG12	42	14.02	TWG42	42	13.82
TWG13	48	15.86	TWG43	48	13.59
TWG14	37	16.05	TWG44	44	14.09
TWG15	39	15.82	TWG45	46	13.70
TWG16	44	15.79	TWG46	45	13.88
TWG17	46	15.34	TWG47	47	13.54
TWG18	48	15.21	TWG48	48	13.54
TWG19	34	15.63	TWG49	34	10.61

Final version is available on: https://doi.org/10.1016/j.jobe.2021.103089

TWG20	37	15.45	TWG50	35	10.39
TWG21	44	15.52	TWG51	42	10.48
TWG22	39	15.52	TWG52	37	11.02
TWG23	46	15.57	TWG53	44	11.09
TWG24	34	16.00	TWG54	34	11.18
TWG25	45	16.36	TWG55	45	11.00
TWG26	47	15.95	TWG56	35	11.09
TWG27	48	15.96	TWG57	37	11.09
TWG28	35	16.27	TWG58	42	10.07
TWG29	37	16.27	TWG59	44	10.09
TWG30	45	16.18	TWG60	45	9.84